NONLINEAR WEIR HYDRAULICS

by

Mitchell R. Dabling

A thesis submitted in partial fulfillment
of the requirements for the degree

of

MASTER OF SCIENCE

in

Civil and Environmental Engineering

Approved:

Blake P. Tullis, Ph.D. Major Professor	Michael C. Johnson, Ph.D., P.E. Committee Member
Paul J. Barr, Ph.D., P.E. Committee Member	Mark R. McLellan, Ph.D. Vice President for Research and Dean of the School of Graduate Studies

UTAH STATE UNIVERSITY
Logan, Utah

2014

ABSTRACT

Nonlinear Weir Hydraulics

by

Mitchell R. Dabling, Master of Science

Utah State University, 2013

Major Professor: Blake P. Tullis
Department: Civil and Environmental Engineering

A hydraulically undersized control structure could result in water overtopping a dam or channel banks. To increase hydraulic capacity and reduce flooding risk, nonlinear spillways are frequently replacing linear weirs. This study investigates four subjects to further knowledge for two types of nonlinear weir, the piano key and labyrinth.

Weir submergence is a condition when the downstream water level of a weir exceeds the weir crest elevation, and can influence the head-discharge relationship of the structure. The effects of submergence on laboratory-scale piano key weir head-discharge relationships were evaluated experimentally and compared to published submergence data for linear and labyrinth weirs. For relatively low levels of submergence, the piano key weir requires less upstream head relative to the labyrinth weir (<6%). This increase in efficiency was reversed at higher levels.

Staged labyrinth weirs feature multiple weir segments with different crest elevations, which confine base flows and/or satisfy downstream discharge requirements.

Head-discharge relationships for various laboratory-scale staged labyrinth weir configurations were established. The accuracy of a head-discharge predictive technique based upon superposition and traditional labyrinth weir empirical data was evaluated, and found to be generally within ±5%.

The influence of linear, labyrinth, and staged labyrinth weir head-discharge characteristics on the outflow hydrograph behavior was evaluated by numerically routing various flood discharges through a fictitious reservoir; peak outflow, maximum water surface elevation, and required detention volume data are presented for each weir alternative. A staged labyrinth weir can be an effective alternative for decreasing the peak outflow hydrograph for frequent events, while increasing discharge for higher return period storm events.

Approach flow perpendicular to the labyrinth weir centerline axis may not be possible in all situations. The head-discharge characteristics of a laboratory-scale labyrinth weir were evaluated with three different approach flow angles (0°, 15°, and 45°). For approach flow angles up to 15°, no measurable loss in discharge efficiency occurred. The discharge efficiency reduced as much as 11% for the 45° approach angle case.

While all data presented are specific to the weir configurations and geometries tested, these data can be beneficial to the general understanding of nonlinear weirs.

(111 pages)

PUBLIC ABSTRACT

Nonlinear Weir Hydraulics

by

Mitchell R. Dabling, Master of Science

Utah State University, 2013

Major Professor: Blake P. Tullis
Department: Civil and Environmental Engineering

A hydraulically undersized control structure (i.e., an emergency dam spillway) could result in water overtopping a dam or riverbanks. To increase hydraulic capacity and reduce flooding risk, nonlinear weirs are being used to replace undersized linear weirs during control structure rehabilitation. The complex geometry of a nonlinear weir creates an infinite number of designs and three-dimensional flow patterns. This study investigates four subjects to further knowledge on two types of nonlinear weir, the piano key and labyrinth.

Weir submergence is a condition when the downstream water level of a weir exceeds the weir crest elevation, and can influence the head-discharge relationship of the structure. The effects of tailwater submergence on laboratory-scale piano key weir head-discharge relationships were evaluated experimentally and compared to previously published data on linear and labyrinth weir submergence. The results of this comparison show that for relatively low levels of submergence, the piano key weir requires

marginally less upstream head relative to the labyrinth weir to pass a given flow (<6%). This increase in efficiency was reversed at higher submergence levels.

Staged labyrinth weirs feature multiple weir segments of differing crest elevations, which confine base flows to a subset of the spillway and/or satisfy downstream discharge hydrograph requirements. The flow characteristics of various laboratory-scale staged labyrinth weir configurations were tested. Head-discharge relationships were established, and the accuracy of a head-discharge predictive technique based upon superposition (i.e., calculating the discharge contribution of each weir segment individually and summing) and traditional labyrinth weir empirical data was evaluated. Relative to the experimental results, the superposition technique estimations were generally within ±5% for all configurations tested except at lower headwater depths where maximum estimation errors occurred (maximum of 15%). When discharge was limited to the lower stage weir segment, the predictive discharge errors were up to 20% for some notch configurations.

The influence of linear, labyrinth, and staged labyrinth weir head-discharge characteristics on the outflow hydrograph behavior was evaluated by numerically routing various flood discharges through a fictitious reservoir; peak outflow discharges, the maximum water surface elevation, and the required detention volumes were quantified and are presented for each weir alternative. A staged labyrinth weir can be an effective alternative for modifying (decreasing) the peak outflow hydrograph for frequent events, while increasing discharge (through effective utilization of the reservoir flood-routing detention volume) for higher return period storm events.

For labyrinth weirs in reservoir applications, approach flow perpendicular to the labyrinth weir centerline axis may not be possible in all situations. The head-discharge characteristics of a laboratory-scale 4-cycle, 15° labyrinth weir with a channelized approach flow were evaluated with three different approach flow angles (0°, 15°, and 45°). The experimental data were also compared with the head-discharge characteristics of a prototype labyrinth weir model study that featured significant approach flow angles. For approach flow angles up to 15°, no measurable loss in discharge efficiency occurred. The discharge efficiency reduced by as much as 11% for the 45° approach flow angle case. The skewed approach flow angle produced unique flow patterns in the labyrinth cycles and on the downstream spillway apron.

While all data presented are specific to the weir configurations and geometries tested, these data can be beneficial to the general understanding of nonlinear weirs.

– Mitchell Dabling

ACKNOWLEDGMENTS

This thesis is the culmination of nearly three and a half years of research at the Utah Water Research Laboratory at Utah State University. As I look back on my time here, I realize that there are many individuals who have influenced and encouraged me. It would be too difficult to list each by name, but I am grateful for each one of you.

This research would not be possible without my major professor, Dr. Blake Tullis. I'll always remember when I was first offered a research position by Blake as we were returning home from a humanitarian trip to Peru. That plane ride changed my degree emphasis, career goals, and my life. While working with Blake we have traveled to conferences around the world together, ventured back to Peru for another humanitarian trip, and developed a friendship that I will always cherish. He has been a friend, mentor, counselor, and leader to me.

I am also deeply grateful for my parents, Robby and Cindy Dabling. They put up with me for 18 years before I headed up to Utah State, and instilled in me a love of God, a strong work ethic, honest morals, and a drive to succeed. I owe them everything I have and ever will accomplish. Because of their example throughout my life, I strive to always be the best version of me.

I may have never developed a passion for research without the guidance and direction of Dr. Joyce Kinkead. When I was accepted to Utah State I was also granted the Undergraduate Research Fellowship. This award required me to become involved in research throughout my undergraduate career, something that most students never take the opportunity to do. The untold story is that I was originally denied this scholarship

(perhaps based on a poor choice of tie color for the interview), but Joyce changed the decision and accepted me into the program. Without this, I may have never gained the desire to pursue graduate education.

Finally, I would like to thank all of my committee, fellow water lab students, Utah State professors, UWRL staff and the "shop guys." There is a lot of work involved with education and research, much of which largely goes unnoticed, vital for enabling students to succeed. I am grateful for each one of you I have met during my five years at USU.

– Mitch

CONTENTS

Page

ABSTRACT iii

PUBLIC ABSTRACT v

ACKNOWLEDGMENTS viii

LIST OF TABLES xii

LIST OF FIGURES xiii

NOTATIONS xvi

CHAPTER

I INTRODUCTION 1

II PIANO KEY WEIR SUBMERGENCE IN CHANNEL APPLICATIONS 6

Abstract 6
Introduction 6
Background 9
Experimental Method 12
Experimental Results 15
Conclusions 19

III STAGED LABYRINTH WEIR HYDRAULICS 22

Abstract 22
Introduction 23
Experimental Setup 26
Experimental Results 28
Conclusions 37

Page

IV MODIFYING THE DOWNSTREAM HYDROGRAPH WITH STAGED LABYRINTH WEIRS 39

Abstract 39
Introduction 40
Numerical Model Setup 43
Experimental Results and Discussion 45
Conclusions 50

V LABYRINTH WEIR HYDRAULICS WITH ANGLED APPROACH FLOW 53

Abstract 53
Introduction 54
Experimental Setup 57
Experimental Results 57
Conclusions 62

VI CONCLUSIONS 64

REFERENCES 68

APPENDICES 71

Appendix A – Submerged Piano Key Weir Data 72
Appendix B – Staged Labyrinth Weir Data 79
Appendix C – Angled Approach Flow Data 87
Appendix D – Permissions 91

LIST OF TABLES

Table		Page
1	Empirical Relationships for Predicting Submergence-Influenced Upstream Head (H^*) as a Function of H_d and H_o for Sharp-Crested Linear Weirs and Labyrinth Weirs (Tullis et al. 2007)	11
2	Piecewise $H^*/H_o = f(H_d/H_o)$ Functions for Standard and Modified Piano Key Weirs	18
3	Laboratory Model Test Matrix	27
4	Coefficients for Eq. (5)	32
5	Maximum Superposition Error for Ranges of H_t/P	34
6	Discharge and Storage Data	47
7	Trend Line Equation Coefficients [Eq. (9)]	59

LIST OF FIGURES

Figure		Page
1	Staged labyrinth weir at Upper Owl Creek Dam, Tamaqua, PA	2
2	Staged labyrinth weir at Leaser Lake Dam, Fogelsville, PA	3
3	Staged labyrinth weir at Lake Townsend Dam, Greensboro, NC	4
4	Piano key weir under submerged and free-flow conditions	7
5	Examples of weirs with the same footprint: (a) piano key; (b) labyrinth	9
6	Dimensional overviews of test weirs: (a) standard piano key; (b) modified piano key	13
7	Three-dimensional renderings of test weirs: (a) standard piano key; (b) modified piano key	13
8	Overview photos of modified piano key weir for $H_o/P = 0.2$: (a) under free-flow conditions; (b) submerged ($S = 0.96$)	15
9	Standard piano key weir H^*/H_o versus H_d/H_o submergence data	16
10	Modified piano key weir H^*/H_o versus H_d/H_o submergence data	17
11	H^*/H^* Labyrinth versus S	20
12	Plan (a) and elevation (b) views of labyrinth weir with geometric and hydraulic variables	23
13	Staged labyrinth spillway at Lake Townsend, Greensboro, NC, USA (Photo taken by Brian Crookston)	26
14	Schematic of tested weir configurations	27
15	Illustration of hydraulic parameters associated with (a) weir flow isolated to the low stage and (b) over the entire weir	30
16	$Q_{predicted}/Q_{actual}$ vs. H_t/P data ($Q_{predicted}$ calculated using the superposition method)	30

Figure Page

17 C_d vs. H_t/P for discharges limited to the lower staged section(s) 33

18 Staged labyrinth weir $Q_{predicted}/Q_{actual}$ vs. H_t/P data ($Q_{predicted}$ calculated using the superposition method) 35

19 Flow separation at stage transition of sidewall (Model 4) 36

20 Geometric variables of labyrinth and staged labyrinth weirs in (a) plan and (b) elevation view 40

21 Photos of staged ogee-crested weir (Tom Miller Dam, TX) and staged labyrinth weir (Lake Townsend, NC). Courtesy of: Michael Johnson and Brian Crookston 42

22 Spillway-specific outflow hydrographs for inflow hydrograph-PMF (peak inflow = 300 m^3/s) 46

23 Spillway-specific outflow hydrographs for inflow hydrograph-500 (peak inflow = 75 m^3/s) 46

24 Spillway-specific outflow hydrographs for inflow hydrograph-100 (peak inflow = 37.5 m^3/s) 46

25 Water elevation for hydrograph-PMF (peak inflow = 300 m^3/s) 48

26 Water elevation for hydrograph-500 (peak inflow = 75 m^3/s) 48

27 Water elevation for hydrograph-100 (peak inflow = 37.5 m^3/s) 48

28 Geometric design and discharge parameters of labyrinth weirs 55

29 Overhead view spillway model study with a significant approach flow angle 56

30 Angled approach flow test configurations for (a) $\beta = 0°$, (b) $\beta = 15°$, and (c) $\beta = 45°$ 56

31 Head-discharge data for tested physical models compared to Crookston (2010) 59

32 %Difference of $\beta = 45°$ curve compared to perpendicular approach flow curve 60

Figure Page

33 Flow conditions for $\beta = 45°$, showing imbalance at (a) $H_t/P = 0.5$ and (b) $H_t/P = 1.0$ 61

34 Prototype model study data comparison 62

NOTATIONS

A = apex width;

α = labyrinth weir sidewall angle;

β = angle of approach flow;

C = dimensional discharge coefficient used in the contracted weir equation;

C_d = dimensionless discharge coefficient;

ΔP_{stage} = depth of stage;

g = gravitational constant;

h = piezometric head relative to the normal weir crest elevation;

h_o = piezometric head during free-flow conditions relative to the normal weir crest elevation;

h^* = piezometric head during submerged conditions relative to the normal weir crest elevation;

h' = piezometric head relative to the notched weir crest elevation;

H_d = total downstream head measured relative to the weir crest;

H_o = total upstream head of a weir during free-flow conditions relative to the crest elevation;

H_t = total upstream head of a weir relative to the normal weir crest elevation;

H_t' = total upstream head of a weir relative to the notched weir crest elevation;

H^* = total upstream head of a submerged weir relative to crest elevation;

i = number of contractions in weir;

I = reservoir inflow;

L = weir centerline crest length;

$L_{c\text{-cycle}}$ = weir centerline crest length of one cycle;

l_c = weir sidewall centerline length

l_{stage} = centerline crest length of notch/stage;

N = number of labyrinth weir cycles;

O = reservoir outflow;

P = weir wall height;

P' = weir height of staged section;

Q = flow;

Q_1 = discharge associated with driving head H^*;

Q_{actual} = experimentally determined discharge;

$Q_{predicted}$ = weir discharge predicted using superposition method;

Q_s = difference between the free-flow discharge associated with h^* and the free-flow discharge associated with h_d;

R_{crest} = weir crest radius;

S = submergence factor (H_d /H^*);

S' = reservoir storage;

t_s = thickness of vertical weir walls;

V = average flow velocity;

w = weir cycle width;

W = channel width at the weir location

CHAPTER I

INTRODUCTION

Dams and hydraulic control structures are critical infrastructure throughout the world, managing water for flood control, irrigation storage, culinary supply, and recreation. One relatively common hydraulic structure is the weir, which is often used as a control structure for in-stream applications or reservoir spillways. Uses for weirs include flow measurement in a channel, flow diversion for irrigation, and flooding control during large storm event (e.g. a probable maximum flood). Weirs can be used as an active or passive control structure (with or without gates), but must be designed to operate safely throughout the range of predicted design flood conditions.

Relative to traditional linear weirs (e.g., ogee crest), nonlinear weirs can increase the flow capacity in discharge channels of limited width without increasing the upstream head required. Linear and nonlinear weirs refer to the layout of the weir wall(s) in plan view. Typical nonlinear weirs include labyrinth and piano key (PK) weirs. Their use is becoming more common, especially for spillway rehabilitation throughout the world (see Figs. 1-3). A short list of some labyrinth weirs in the United States includes:

- 19th Street Labyrinth Weir Dam – San Antonio, TX
- Huntington Hills Lake – Anderson, SC
- Lake Townsend Dam – Greensboro, NC
- Lake Brazos Dam – Waco, TX

Fig. 1. Staged labyrinth weir at Upper Owl Creek Dam, Tamaqua, PA

- Leaser Lake Dam – Fogelsville, PA
- New London Dam – New London, MN
- South Holston Lake – Abingdon, VA
- Upper Owl Creek Dam – Tamaqua, PA
- Isabella Dam – Kernville, CA (in design phase)
- Millsite Reservoir – Ferron, UT (in design phase)

As new technology is implemented, research must continue to push current knowledge. The hydraulic properties of nonlinear weirs are very complex. Three-dimensional flow patterns and the infinite number of configurations possible increase the

Fig. 2. Staged labyrinth weir at Leaser Lake Dam, Fogelsville, PA

difficulty of fully understanding how labyrinth and piano key weirs will operate. The goal of this study is to investigate four areas of non-linear weir hydraulics:

1. Discharge characteristics of piano key weirs with tailwater submergence
2. Discharge characteristics of staged (notched) labyrinth weirs
3. Modifying the outflow hydrograph of a reservoir using staged labyrinth weirs
4. Discharge efficiency of labyrinth weirs with an angled approach flow

These studies were selected because of their relative lack of previous research and impact on general nonlinear weir knowledge.

Piano Key Weirs

The Piano Key (PK) weir is essentially a rectangular labyrinth weir with cantilevered upstream and/or downstream apexes and ramped floors in the inlet and outlet cycles or keys. The PK weir's cantilevered apexes help to produce a longer weir crest length relative to a rectangular labyrinth weir with the same footprint.

The PK weir's reduced footprint relative to its crest length makes it particularly well suited for spillway applications with limited footprint space (i.e., on top of a narrow concrete gravity dam). In addition to the top-of-dam applications, recent interest has focused on using PK weirs in river and channel applications. When deciding between a labyrinth and a PK weir for a channel application, the potential influence of submergence, along with the free-flow discharge capacity of both weirs, must be

Fig. 3. Staged labyrinth weir at Lake Townsend Dam, Greensboro, NC

considered, but little information has been published on the submergence effects of PK weirs.

Labyrinth Weirs

The replacement of linear weirs with nonlinear weirs (labyrinth weirs in many cases) is often considered as an alternative for increasing spillway discharge capacity without increasing the existing spillway channel width. The geometry of a labyrinth weir can significantly increase the crest length within a given channel width relative to a linear weir. Because this increased crest length can improve hydraulic performance, labyrinth weirs have been of interest to practitioners and researchers for many years.

In addition to passing the more extreme flood events [e.g., the Probable Maximum Flood (PMF), 500-year flood, etc.], an upgraded hydraulically more efficient spillway design may also be required to limit spillway discharges to pre-development peak outflows for the more frequent return-period storm events to satisfy downstream flood-control regulations. A labyrinth weir that incorporates weir segments with different elevations (i.e., staged labyrinth weir) is one method of reducing the peak outflow discharge for frequent return-period storm regulations, while still providing sufficient discharge capacity to pass larger storm events.

CHAPTER II

PIANO KEY WEIR SUBMERGENCE IN CHANNEL APPLICATIONS[†]

Abstract

Weir submergence can influence head-discharge relationships for weirs used in channel applications when high tailwater conditions exist owing to a downstream control. Weir submergence describes a condition in which the water level downstream of the weir exceeds the weir crest elevation. When a weir becomes submerged, the driving head required to pass a specific discharge over the weir can increase significantly relative to a free-flow condition. In this study, the effects of tailwater submergence on laboratory-scale piano key weir head-discharge relationships were evaluated experimentally and compared with previously published data for labyrinth and sharp-crested linear weir submergence. The results of this comparison show that for relatively low levels of submergence, the piano key weir requires less upstream head relative to the labyrinth weir to pass a given discharge. This increase in efficiency was minimal (< 6%) and was reversed at higher submergence levels.

Introduction

Weirs are commonly used for flow measurement, flow diversion, and/or flow control in canals, rivers, and reservoirs. Although weirs are generally designed to operate under free-flow conditions, they can become submerged under certain conditions. Weir

---

[†] Dabling, M.R., and Tullis, B.P. (2012). "Piano key weir submergence in channel applications." *J. Hydraul. Eng.*, ASCE, 138(7), 661-666.
Used with permission from ASCE (see Appendix D)

submergence occurs when the downstream water level exceeds the crest elevation, a condition that is more common for weirs situated in rivers or canals with a mild slope, flow constrictions, and/or excess in-stream vegetation downstream. Submergence is quantified by the ratio of the total head downstream of the weir to the total head upstream. At low submergence levels, the elevated tailwater does not affect the free-flow total upstream head (H_o), a condition known as modular submergence. When the modular submergence limit is exceeded, the upstream total upstream head (H^*) increases relative to H_o for a given weir discharge (Q), increasing the potential for upstream flooding. Fig. 4 shows the difference between the submerged and free-flow hydraulic parameters.

Relative to traditional linear weirs (e.g., ogee crest), the use of nonlinear weirs to increase the flow capacity in discharge channels of limited width without significantly increasing the required H_o is becoming more common, especially for spillway rehabilitation. Linear and nonlinear weir designations refer to the layout of the weir wall(s) in plan view. Typical nonlinear weirs include labyrinth and piano key (PK) weirs (Fig. 5). The PK weir is essentially a rectangular labyrinth weir with cantilevered upstream and/or down- stream apexes and ramped floors in the inlet and outlet cycles or keys. The PK weir's cantilevered apexes help to produce a longer weir crest length

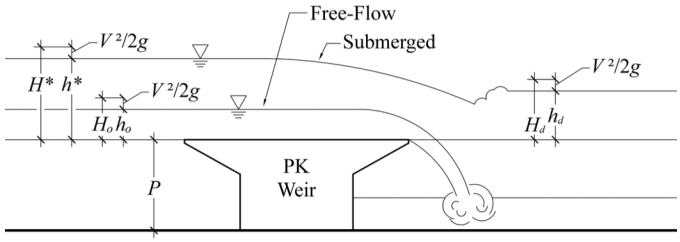

Fig. 4. Piano key weir under submerged and free-flow conditions

relative to a rectangular labyrinth weir with the same footprint.

The PK weir's reduced footprint relative to its crest length makes it particularly well suited for spillway applications with limited footprint space (i.e., on top of a narrow concrete gravity dam). The number of geometric parameters that PK weirs have is significant (see Pralong et al. 2011 for a full description of the PK geometric parameters); the influence of the PK weir geometric parameters on the discharge efficiency, either individually or collectively, is not well understood. On the basis of preliminary testing, however, Lempérière (2009) has recommended a standard PK weir geometry for design. Anderson (2011) found that the PK weir discharge capacity could be improved beyond the standard design by adding various design modifications (e.g., rounded noses on the upstream apexes; a parapet wall on top of the weir; improved crest shapes, such as a half-round).

In addition to the top-of-dam applications, recent interest has focused on using PK weirs in river and channel applications (Ho Ta Khanh et al. 2011). For channel applications without significant weir footprint restrictions, Anderson (2011) found that trapezoidal labyrinth weirs typically provide more discharge capacity per unit weir length than do PK weirs. For cases in which the footprint is constrained in width and/or length, space may be insufficient to accommodate the required labyrinth weir wall length; in such cases, a PK weir would likely produce a higher total weir discharge owing to its compact geometry (large weir length for a given footprint size). Anderson and Tullis (2012) found that a Type-A PK weir was hydraulically more efficient than a rectangular labyrinth weir with the same crest layout (i.e., same crest length and layout in plan view).

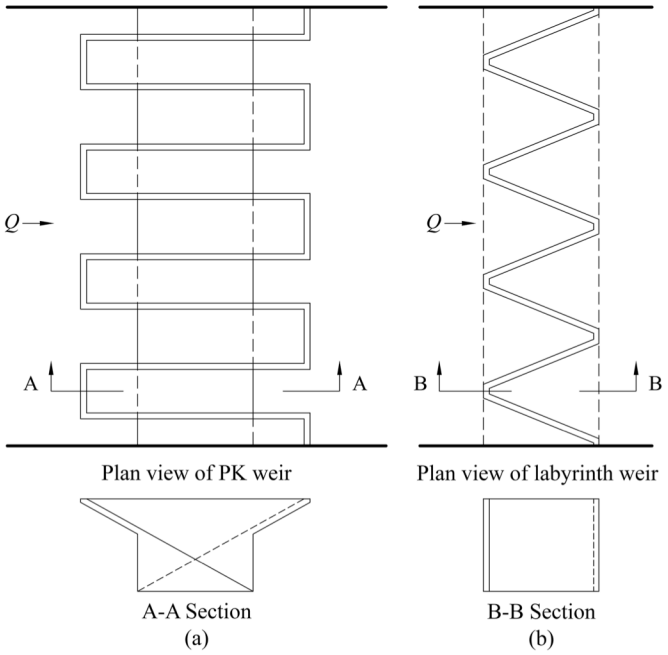

Fig. 5. Examples of weirs with the same footprint: (a) piano key; (b) labyrinth

When deciding between a labyrinth and a PK weir for a channel application, the potential influence of submergence, along with the free-flow discharge capacity of both weirs, must be considered. In this study, the submerged discharge characteristics of PK weirs (with and without modifications) are evaluated and compared with the submergence characteristics of labyrinth and sharp-crested linear weirs.

Background

Little information has been published on the submergence effects of PK weirs. In part, this may be because PK weirs are generally used for top-of-dam applications, in which submergence is typically not a factor. Many researchers, including Fteley and Stearns (1883), Francis (1884), Bazin (1894), Cox (1928), and Villemonte (1947), have studied sharp-crested linear weir submergence and published submergence relationships

on the basis of a flow reduction factor, Q_s / Q_1. Tullis et al. (2007) studied labyrinth weir submergence and compared it with Villemonte's relationship; the results of that study will be compared with the PK weir submergence data from this study.

Weir Basics

In this study, a common form of the weir equation [Eq. (1)] (Henderson 1966) was used to quantify the PK weir head-discharge relationship where g = the gravitational acceleration constant; L = the weir crest length; H_o = free-flow (nonsubmerged) upstream total head (flow depth measured relative to the weir crest elevation plus the approach flow velocity head); and C_d = dimensionless discharge coefficient that varies with weir type, geometry, crest shape, and flow conditions. The total head was used rather than the piezometric head (h_o) to better account for approach flow influences.

$$Q = \frac{2}{3} C_d L \sqrt{2g} H_o^{3/2} \tag{1}$$

Weir Submergence

Submergence (S) is defined as the ratio of the total downstream head (H_d) to the total submerged-flow upstream head (H^*), as shown in Eq. (2). Fig. 4 shows an illustration of submerged and free-flow weir parameters. As H_d increases, H_d approaches H^*; when $H_d = H^*$, the weir no longer acts as a control structure, and $S = 1.0$. Tullis et al. (2007) compared the submergence behavior of labyrinth weirs with the linear weir submergence relationship developed by Villemonte (1947) and found that for the same H_d and Q, labyrinth weirs generally produced a lower H^* than linear weirs.

$$S = \frac{H_d}{H^*} \tag{2}$$

The increased discharge efficiency of the labyrinth weir under submerged conditions means that the extent of upstream flooding during submerged-flow conditions would be less for the labyrinth weir than for the sharp-crested linear weir. The submerged labyrinth weir data were not well represented by Villemonte's sharp-crested linear weir relationship; Tullis et al. (2007) developed a dimensionless piecewise bounding curve relating H_d/H_o (the submerging downstream total head normalized by the free-flow up-stream total head) to H^*/H_o (the submerged upstream total head normalized by the free-flow upstream total head) for labyrinth and sharp-crested linear weirs. Piecewise bounding curve equations for both linear and labyrinth weirs under submerged conditions are shown in Table 1.

Research Objectives

The objectives of this study included evaluating the submerged head-discharge characteristics of standard and modified PK weir geometry; the submerged PK weir

Table 1. Empirical Relationships for Predicting Submergence-Influenced Upstream Head (H^*) as a Function of H_d and H_o for Sharp-Crested Linear Weirs and Labyrinth Weirs (Tullis et al. 2007)

Model	H_o/P	Equation	Bounds
Linear	0.2	$H^*/H_o = 0.2426(H_d/H_o)^2 + 0.0649(H_d/H_o) + 1$	$0 \le H_d/H_o \le 1.78$
		$H^*/H_o = 0.0131(H_d/H_o)^2 + 0.8712(H_d/H_o) + 0.2919$	$1.78 \le H_d/H_o \le 3.5$
		$H^* = H_d$	$3.5 \le H_d/H_o$
Labyrinth	0.2	$H^*/H_o = 0.0322(H_d/H_o)^4 + 0.2008(H_d/H_o)^2 + 1$	$0 \le H_d/H_o \le 1.53$
		$H^*/H_o = 0.9379(H_d/H_o) + 0.2174$	$1.53 \le H_d/H_o \le 3.5$
		$H^* = H_d$	$3.5 \le H_d/H_o$

Note: H_d = total downstream head; H_o = free-flow total upstream head; P = weir height (see Fig. 4).

behavior was also compared with submerged labyrinth and linear weir behavior.

Experimental Method

Testing Apparatus

The PK weir submergence testing was conducted in a laboratory flume measuring 0.93 m wide, 0.61 m deep, and 7.4 m long. Water entered the flume through a head box containing a flow diffuser, a vertical baffle wall, and a floating surface wave suppressor, all of which served to create a relatively uniform approach flow condition. A stilling well with a point gauge (readable to ±0.15 mm) was hydraulically connected to the flume sidewall at a distance of 4P times the weir height, (approximately 0.8 m) upstream of the weir for measuring the piezometric head level (h_o and h^*). A second stilling well with point gauge connected to the flume 10P (approximately 2.0 m) downstream of the weir was used to measure the downstream piezometric head (h_d). Both H_o and H_d were calculated by adding the velocity head ($V^2/2g$) corresponding to the average cross-sectional velocity at the respective measurement locations. For the submergence investigation, variations in tailwater elevation were produced using an adjustable gate located 15P (approximately 3.0 m) downstream of the weir. A calibrated orifice meter [traceable to the National Institute of Standards and Technology (NIST) by weight] located in the 305 mm diameter supply piping was used to accurately measure the weir discharge (± 0.2%).

Weir Design, Construction, and Setup

The submerged head-discharge characteristics were evaluated for two different PK weir geometries, identified as PKst and PKmod. The PKst represents the standard PK weir design recommended by Lempérière (2009) with a flat-top weir crest; the PKmod is the same as the PKst design with the addition of rounded abutments on the upstream apexes and a parapet wall featuring a half-round crest on top of the weir. The PK weirs used in this study are geometrically consistent with two of the models tested by Anderson (2011).

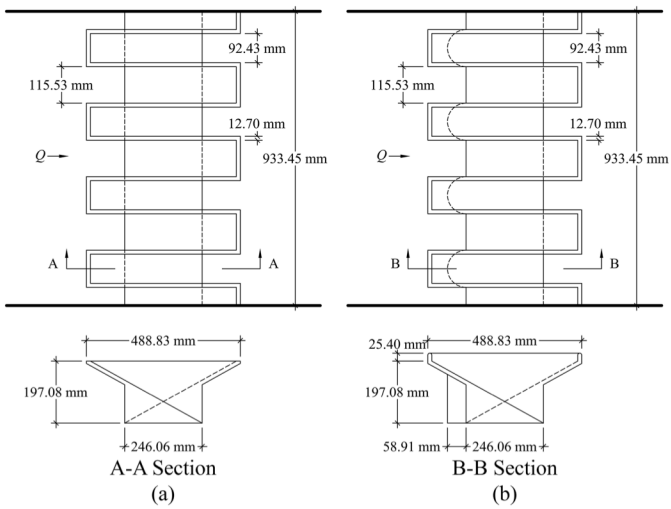

Fig. 6. Dimensional overviews of test weirs: (a) standard piano key; (b) modified piano key

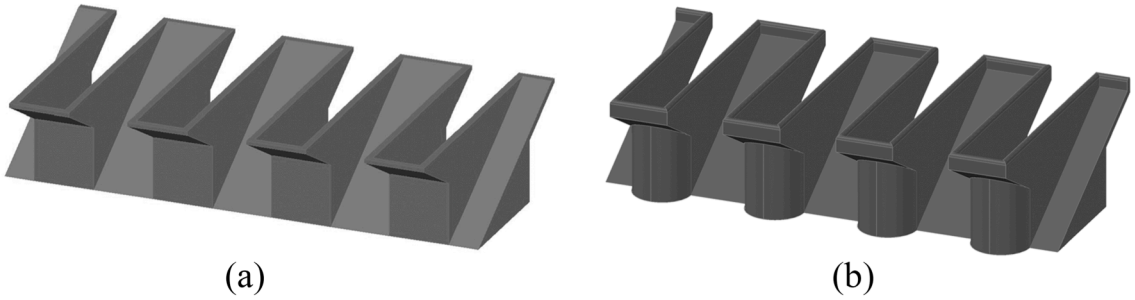

Fig. 7. Three-dimensional renderings of test weirs: (a) standard piano key; (b) modified piano key

The weirs were fabricated using 12.7 mm thick clear acrylic. The thickness-to-weir height ratio ($T_s/P = 15.75$) of the PKst laboratory-scale weir was scaled to be geometrically similar to an existing prototype structure [Goulours Dam (Laugier 2007)]. The weir crests were machined to help with leveling. Figs. 6 and 7 show overviews of the PKst and PKmod weir geometries. The weirs were installed on top of a 63.5 mm tall adjustable platform for leveling purposes (±0.40 mm); a ramp with a slope of 4:1 was used to transition the flow from the floor of the flume to the base of the weir.

Testing Procedure

With the weir installed, the crest length of the weir (L) was measured. Gravity-fed reservoir water with a temperature of 6.4-6.8 °C was used for testing. Water was allowed to flow through the flume for a minimum of 30 minutes before data collection (e.g., measuring weir crest references or head-discharge data) to allow the thermal contraction of the acrylic weir walls to stabilize. Three data sets corresponding to H_o/P values of 0.2, 0.4, and 0.6 were collected for each test weir. These equate to discharge values of 0.053, 0.104, and 0.157 m^3/s for the PKst and 0.067, 0.133, and 0.195 m^3/s for the PKmod weir. Before submergence testing, H_o (free-flow up- stream total head) was determined as a reference for each flow rate tested. After allowing a minimum of 5 minutes for flow conditions to stabilize, H_o (or H^* for submerged conditions) was determined using the upstream point gauge and velocity head data. For submerged weir conditions, H_d was determined at the downstream measurement location. Once the free-flow head-discharge condition was determined, 15-30 different submerged-flow conditions created using the adjustable tailgate were evaluated and documented for each flow rate tested (see

Appendix A). Fig. 8 shows overview photos of the PKmod weir under free-flow and submerged ($S = 0.96$) conditions for $H_o/P = 0.2$.

Experimental Results

Piano Key Weir Submergence

For each submergence test condition, H^* and H_d were nondimensionalized using the corresponding H_o value, consistent with the Tullis et al. (2007) analysis for labyrinth and linear weirs. H^*/H_o versus H_d/H_o data for the PKst and PKmod are shown in Figs. 9 and 10, respectively, as a function of H_o/P. Reference S values are also shown in Figs. 9 and 10. The data shown in Figs. 9 and 10 are limited to $H_d/H_o \leq 3.0$ to improve visual clarity between data sets; the study evaluated H_d/H_o values tested up to ~3.9. Trend lines were generated for each test condition. Although the H_o/P-specific trend lines had very similar shapes, the data in Figs. 9 and 10 show that the relationship between H^* and H_d, when nondimensionalized by H_o, are H_o/P (i.e., flow rate) dependent. As H_o/P increased, both the PKst and PKmod weirs were less responsive to submergence (H^*/H_o

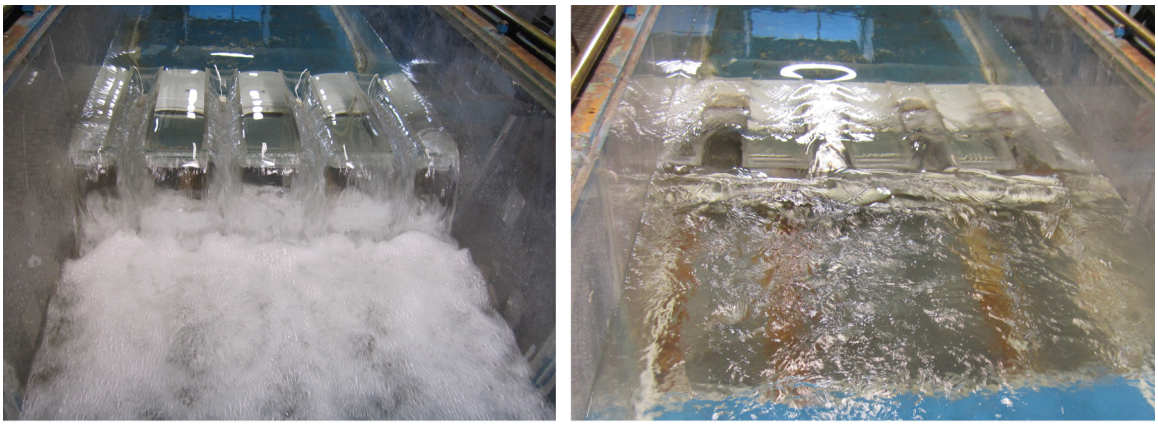

(a) (b)

Fig. 8. Overview photos of modified piano key weir for $H_o/P = 0.2$: (a) under free-flow conditions; (b) submerged ($S = 0.96$)

was lower at corresponding values of H_d/H_o). The data in Figs. 9 and 10 also show that $H^* \approx H_o$ for $S < \sim 0{:}48$ (modular submergence range); this means that tailwater submergence effects do not begin to influence the free- flow head-discharge relationship until the tailwater total head exceeds 48% of the upstream total head. As the submergence level for PK weirs increases, the weirs will eventually stop functioning as a head-discharge control as the flow condition approaches full- submergence ($H_d = H^*$; $S = 1.0$). This occurs at lower H_d/H_o values as H_o/P increases. It was also observed that the PKst reaches full-submergence at a smaller H_d/H_o value than the PKmod.

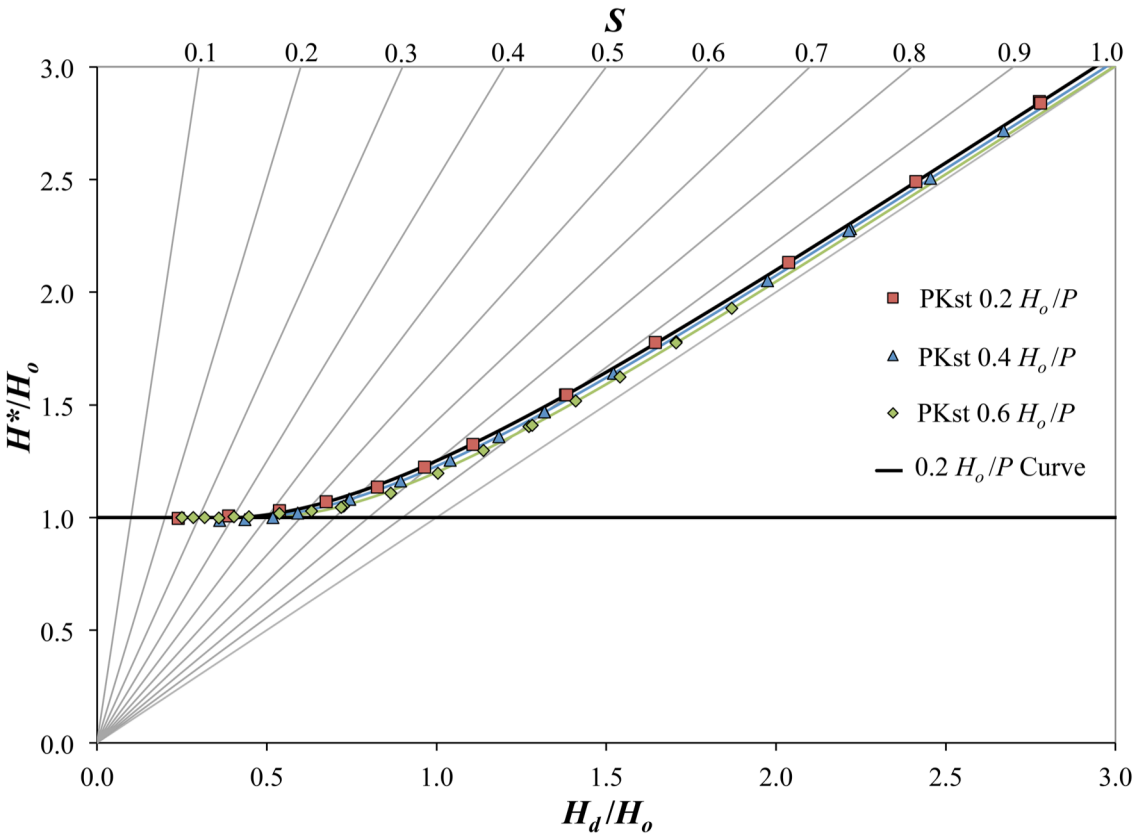

Fig. 9. Standard piano key weir H^*/H_o versus H_d/H_o submergence data

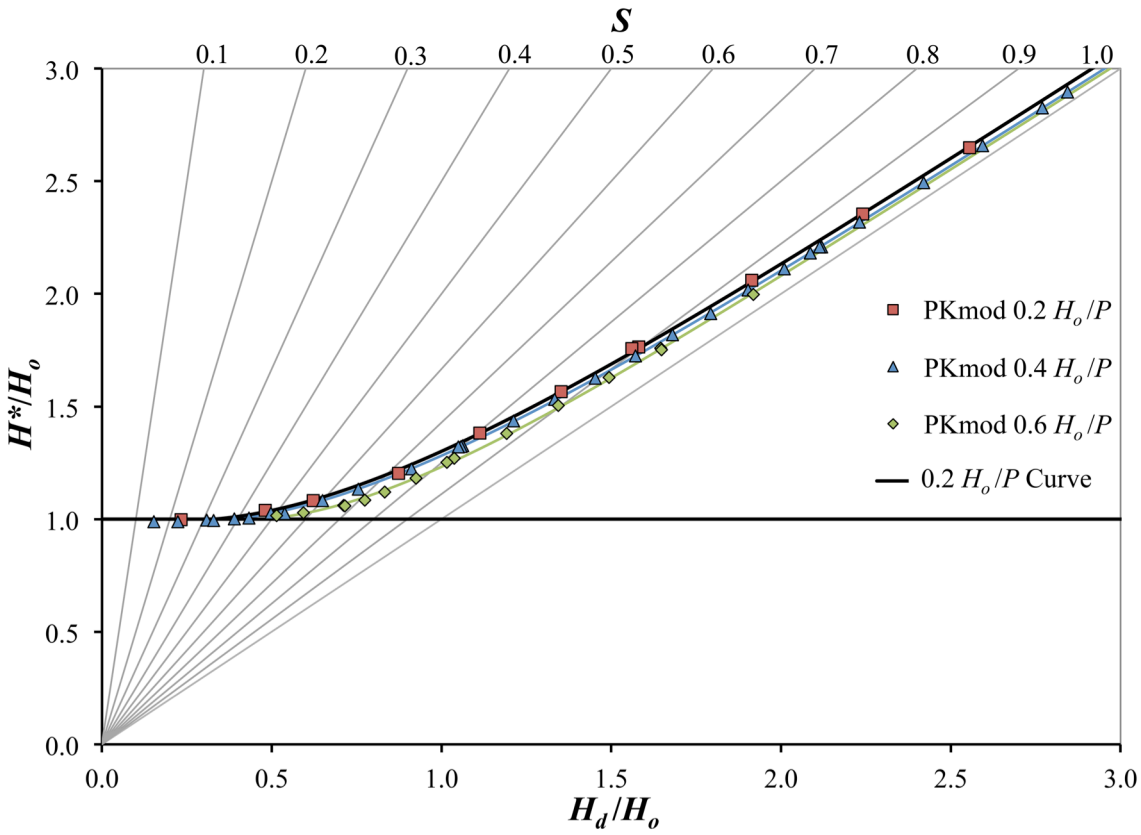

Fig. 10. Modified piano key weir H^*/H_o versus H_d/H_o submergence data

When using the data in Figs. 9 and 10 for design purposes, it is important to remember that the data are H_o/P specific. A piecewise function [Eq. (3)] was fit to the $H_o/P = 0.2$ trend line ($R^2 = 0.9999$) with the corresponding empirical coefficients shown in Table 2. This H_o/P condition represents a bounding curve because it corresponds to the most conservative of the data sets (largest H^* for a given H_d, as shown in Figs. 9 and 10) of the H_o/P conditions tested. However, the $H_o/P = 0.2$ curve may be nonconservative for discharges that correspond to $H_o/P < 0.2$, and the $H_o/P = 0.4$ and 0.6 data may be more appropriate for higher discharge applications.

$$\frac{H^*}{H_o} = A\left(\frac{H_d}{H_o}\right)^B + Ce^{D(H_d/H_o)} \quad (3)$$

The dimensionless submerged total head PK weir curves [Eq. (3); Table 2] are compared with the equivalent submerged labyrinth weir relationships presented by Tullis et al. (2007) (Table 1) in Fig. 10. The submerged PK H^* data were normalized by the submerged labyrinth H^* data and plotted as a function of S. For smaller S values, the PK weirs were less susceptible to submergence effects [i.e., smaller H^* (or H^*/H_o) values are produced for a given S, relative to labyrinth weirs]. This effect is reversed at higher values of S, at which the submerged PK weirs become less efficient than the labyrinth weir [i.e., higher PK weir H^* (or H^*/H_o) value than the labyrinth weir at the same S value]. Even values of S exist at which the H^* for the PK weir is more submergence-

Table 2. Piecewise $H^*/H_o = f(H_d/H_o)$ Functions for Standard and Modified Piano Key Weirs

Model	H_o/P	Equation or coefficients for Eq. (2)	Bounds
PKst	0.2	$H^*/H_o = 1$	$0 \le H_d/H_o < 0.42$
		$A = 1.0615$ $B = 0.96121$ $C = 1.1454$ $D = -1.7951$	$0.42 \le H_d/H_o \le 4.66$ $R^2 = 0.99999$
		$H^* = H_d$	$4.66 < H_d/H_o$
PKmod	0.2	$H^*/H_o = 1$	$0 \le H_d/H_o < 0.34$
		$A = 1.0731$ $B = 0.95659$ $C = 1.0353$ $D = -1.5134$	$0.34 \le H_d/H_o \le 5.09$ $R^2 = 0.99997$
		$H^* = H_d$	$5.09 < H_d/H_o$

Note: H^* = submergence-influenced upstream head; H_d = total downstream head; H_o = free-flow total upstream head; P = weir height; A, B, C, and D = empirical coefficients from Eq. (3).

sensitive than the linear weir. Relative to the labyrinth weir submergence behavior, the range of H_d/H_o for which the PK weir was less sensitive to submergence effects increased with increasing H_o/P.

An interesting anomaly was observed during the testing of the PK weir with and without modifications. When the downstream head was very close to but just above the crest elevation, H^* decreased relative to H_o, suggesting that a small increase in discharge efficiency occurs as the PK weir transitions between free-flow and modular submergence. Belaabed and Ouamane (2011) noted a similar observation.

Conclusions

The purpose of this study was to characterize the submerged head-discharge characteristics for PK weirs and compare them with submerged labyrinth weir behavior. Two conservative empirical equations were presented for use in the design of submerged PK weirs. Using the dimensionless-head submergence curves produced, the value of H^* can be estimated for a given value of Q (and corresponding H_o) and H_d. On the basis of the results of this study, the following can be concluded:

- Relative to the sharp-crested linear and labyrinth weir dimensionless submerged-head relationships presented by Tullis et al. (2007) and to each other, the PK weirs tested (PKst, PKmod) produced unique dimensionless submerged-head characteristics that were H_o/P (i.e., discharge) specific.
- The PK weir modular submergence range (a condition in which the tailwater exceeds the weir crest but the free-flow head-discharge relationship still applies)

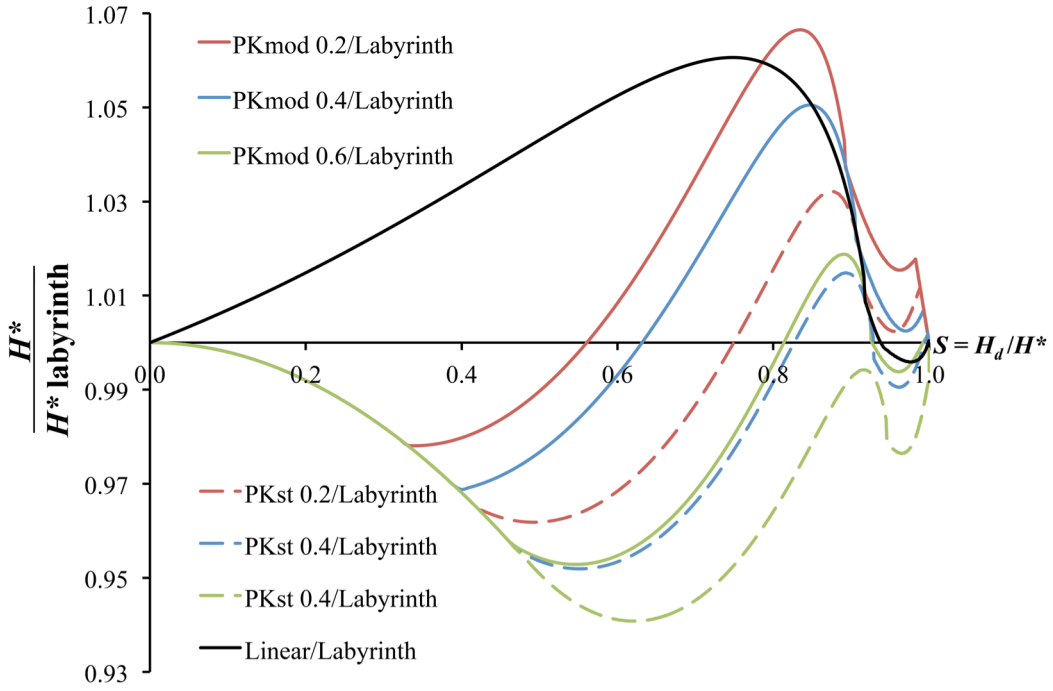

Fig. 11. H^*/H^* Labyrinth versus S

corresponded to $S < \sim 0.48$. A slight increase in weir discharge efficiency relative to the free-flow head-discharge condition was observed for S just greater than 0.

- The PKmod required a larger H^* than the PKst for given normalized downstream head (i.e., H_d/H_o), indicating a higher susceptibility to submergence effects.
- Although minor, both weirs tested were hydraulically more efficient (~6% maximum) than the labyrinth weir at relatively low levels of submergence ($S < 0.55$). This effect is reversed at higher submergence levels. The hydraulic efficiency of the submerged PKst weir exceeded that of the PKmod weir.
- For both the PKst and PKmod, as H_o/P increased, the modular submergence range also increased.

The results presented in the study do not account for any size-scale effects, if any, that may exist between the model and typical prototype size scales. In addition to investigating potential size-scale effects, possible areas of future nonlinear weir submergence research include a comparison with different types of labyrinth weirs and the effects of different PK inlet/outlet cell widths on submergence.

CHAPTER III

STAGED LABYRINTH WEIR HYDRAULICS[‡]

Abstract

Labyrinth weirs with multiple crest elevations (i.e., staged labyrinth weirs) can be used in spillway design to confine base flows to a section of the crest and/or satisfy discharge hydrograph requirements. However, inadequate hydraulic design information is available specific to staged labyrinth weirs. In this study, the flow characteristics of various staged labyrinth weir configurations (laboratory-scale) were tested. Observations of staged labyrinth weir flow characteristics are presented. The influences of the lower stage length, depth, and location on discharge were studied and head-discharge relationships were experimentally determined. The accuracy of a head-discharge predictive technique based upon superposition and traditional labyrinth weir empirical data was also evaluated. Relative to the experimental results, the superposition technique estimations were generally within ±5% for all configurations tested except at lower headwater depths, where maximum estimation errors occurred (maximum of 15%). When discharge was limited to the lower stage weir segment, the predictive discharge errors were up to 20% for some notch configurations. This indicates the discharge of the lower stage segment is location-specific due to the complexity of the labyrinth weir geometry.

[‡] Dabling, M.R., Tullis, B.P., and Crookston, B.M. (2013). "Staged labyrinth weir hydraulics." *J. Irrig. Drain. Eng.*, ASCE, 139(11), 955-960.
Used with permission from ASCE (see Appendix D)

Introduction

Labyrinth Weirs

Dams represent a critical infrastructure component throughout the world. They provide water supply (municipal, agricultural, industrial), flood control, hydropower, navigation, and recreation. Aging infrastructure, changes in land use, and higher peak flow predictions for extreme flood events often require upgrading or rehabilitating existing spillways. The replacement of linear weirs with nonlinear weirs (labyrinth weirs in many cases) is often considered as an alternative for increasing spillway discharge capacity without increasing the existing spillway channel width.

Geometric variables for labyrinth weir design are shown in Fig. 12, where P is the weir height, α is the sidewall angle, A is the apex width, w is the cycle width, and l_c is the sidewall centerline length. The geometry of a labyrinth weir can significantly increase the crest length within a given channel width relative to a linear weir; the additional crest length can increase discharge capacity by 3 to 4 times (Tullis et al. 1995). As a result of their hydraulic performance, labyrinth weirs have been of interest to practitioners and

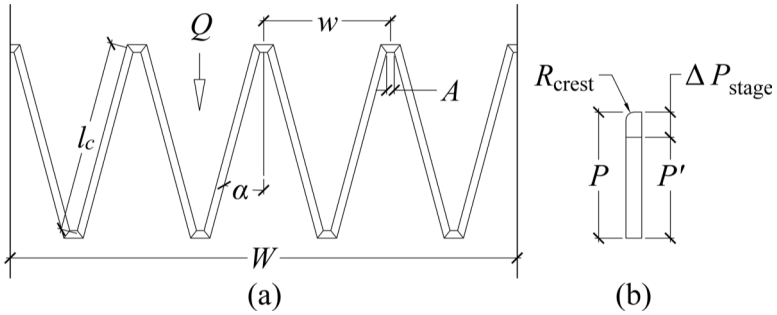

Fig. 12. Plan (a) and elevation (b) views of labyrinth weir with geometric and hydraulic variables

researchers for many years. Notable labyrinth weir design publications that have focused on discharge performance include Hay and Taylor (1970), Darvas (1971), Hinchliff and Houston (1984), Lux and Hinchliff (1985), Magalhães and Lorena (1989), Tullis et al. (1995), Melo et al. (2002), Falvey (2003), Tullis et al. (2007), Crookston (2010), and Crookston and Tullis (2012a, b; 2013a, b). Labyrinth weirs have been used successfully to increase spillway capacity and manage upstream flooding for low probability storm events; however, reservoir outflow hydrographs for more frequent storms may also require consideration.

The increased hydraulic capacity of a labyrinth spillway can decrease reservoir flood wave attenuation and increase the peak outflows associated with inflow hydrographs, potentially increasing downstream flooding for moderate to extreme storm events (Paxson et al. 2011). Therefore, in addition to spillway hydraulic requirements for the design storm (e.g., passing the full PMF), an upgraded, higher flow capacity spillway may require specific design components to generally match pre-development peak outflows for more frequent storm events. For example, a new spillway may be required to pass an enlarged PMF but the 25- and 100-year post-development peak outflows must be less than or equal to those of the existing spillway.

Different spillway types installed in parallel (e.g., gated and ungated spillways) can be an effective means of meeting a prescribed outflow hydrograph requirement during flood routing events. Indeed, the concept of using parallel passive spillway control structures of varied hydraulic characteristics to regulate the outflow hydrograph can also

be applied to labyrinth weirs by incorporating multiple crest elevations – creating a staged labyrinth weir.

Staged Labyrinth Spillways

In the literature and in practice, the terms "notch" and "stage" are often used interchangeably. For weirs with segments at different crest elevations, "stage" refers to a continuous section of weir with a common crest elevation. Because this study focuses on labyrinth weirs with two crest elevations, the term "high stage" and "low stage" are used. A variety of staged weir spillway types [e.g., linear weirs (Piute Dam, Piute County, UT, USA), ogee spillways (Tom Miller Dam, Austin, TX, USA), and labyrinth spillways (Lake Townsend Dam, Greensboro, NC, USA)] have been designed and built featuring segments with different crest elevations. Labyrinth weir stages can consist of full or partial cycle segments. A lower stage may be set at the normal pool elevation and convey base flows and runoff from relatively frequent storm events (e.g., up to the 2-year, 10-year, etc.). The higher stage would provide additional required discharge capacity during more extreme flood events. When staged, labyrinth spillways typically feature two or perhaps three crest elevations, but more elevations can be used depending on the application. Having distributed staged segments at a common elevation (e.g., on each downstream apex) is not uncommon.

Confining base flow and smaller storm event outflows to staged sections can be beneficial for several reasons. Concentrating smaller discharges to shorter weir segments helps to create a thicker nappe, which can potentially reduce the occurrence of nappe vibration. Flow confinement can also limit algal or other biological growth that can

Fig. 13. Staged labyrinth spillway at Lake Townsend, Greensboro, NC, USA (Photo taken by Brian Crookston)

develop on wet surfaces, reducing weir maintenance costs. The recently constructed Lake Townsend Dam (see Fig. 13) features a 7-cycle staged labyrinth spillway; the low stage is comprised of 2 cycles approximately 0.3 m lower than the upper five cycles.

As previously noted, multiple hydraulic design methods have been published for labyrinth weirs; however, no method includes design information specific to staged labyrinth weirs. Practicing engineers would benefit from such information, as it would facilitate more accurate stage-discharge relationship estimations for design. The objective of this study was to investigate the hydraulic performance of staged labyrinth weirs as a function of the staged wall height offset (ΔP_{stage}), stage length (l_{stage}), and location. Geometric variables specific to staged labyrinth weirs are presented in Fig. 12. Using laboratory-scale models, head-discharge data were collected for various staged labyrinth weir configurations.

Experimental Setup

Investigations were conducted in a rectangular flume (1.2 m x 14.6 m x 1.0 m deep) at the Utah Water Research Laboratory (UWRL) at Utah State University. A 4-

cycle ($N = 4$), 15° sidewall angle ($\alpha = 15°$) labyrinth weir with a quarter-round crest shape [$R_{crest} = 1/2$ the wall thickness (t_w)] was tested with the following low stage configurations (see Fig. 14): each downstream apex wall (Models 1a, 1b), centered on a single upstream apex (Model 2), centered on a single downstream apex (Model 3), centered on a single sidewall (Model 4), and a full cycle (Model 5). A standard labyrinth weir with a constant crest elevation (Model 6) was also tested.

All model labyrinth weirs featured the same total weir centerline length (L) and a quarter-round crest shape, with the exception of Models 1a and 1b, in which l_{stage} was

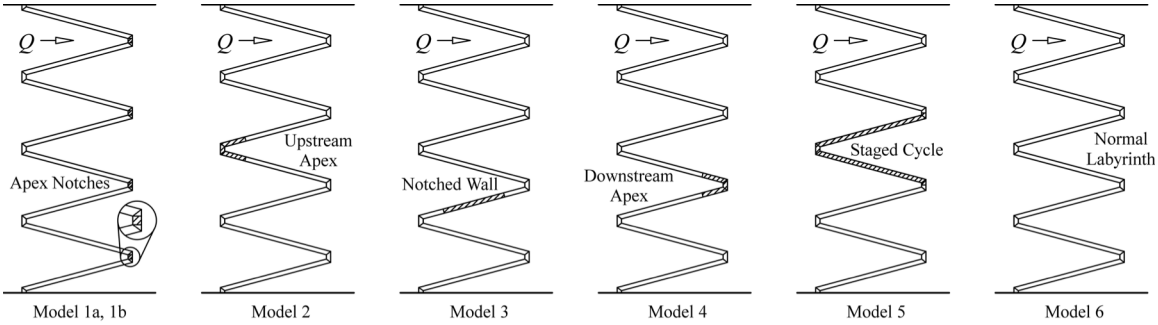

Fig. 14. Schematic of tested weir configurations

Table 3. Laboratory Model Test Matrix

Labyrinth Geometry	Model (#)	Location of Low Stage	Stage Geometry		
			l_{stage}	ΔP_{stage}	Low Stage Crest Shape*
$\alpha = 15°$	1a	Downstream Apexes	18.4 mm x 4	0.2P	Flat
$N = 4$	1b	Downstream Apexes	18.4 mm x 4	0.1P	Flat
$L = 3982.8$ mm	2	Centered on Upstream Apex	232.6 mm	0.2P	QR
$L_{c\text{-cycle}} = 995.7$ mm	3	Centered on Sidewall	232.6 mm	0.2P	QR
$P = 152.4$ mm	4	Centered on Downstream Apex	232.6 mm	0.2P	QR
$w = 305.9$ mm	5	Full Cycle	995.7 mm	0.2P	QR
$t_w = 18.4$ mm	6	Standard Labyrinth	N/A	N/A	QR

*QR = Quarter Round where $R_{crest} = 1/2\ t_w$; Flat = flat-top crest shape

Note: α = labyrinth weir sidewall angle; N = number of labyrinth weir cycles; L = weir centerline crest length; $L_{c\text{-cycle}}$ = weir centerline crest length of one cycle; P = weir height; w = cycle width of weir; t_w = wall thickness of weir; l_{stage} = centerline crest length of low stage; ΔP_{stage} = depth of stage; R_{crest} = weir crest radius.

limited to the downstream inside apex width (A) and featured flat-topped crest shapes. For Model 1b, ΔP_{stage} was 10% of the weir height (i.e., 0.1P), while in Models 1a and 2-5 $\Delta P_{stage} = 0.2P$. For Models 2, 3, and 4, l_{stage} equaled one half of l_c and was centered on an upstream apex, sidewall, or downstream apex, respectively. In Model 5, a full labyrinth weir cycle was lowered [i.e., $l_{stage} = L_{c\text{-cycle}}$ (the cycle centerline crest length)]. The test matrix is summarized in Table 3.

Experimental Results

Head-discharge Performance

Eq. (4), a form of the standard weir equation (Henderson 1966), was selected to quantify the head-discharge relationship of the tested physical models and to calculate discharge coefficients for varying flow conditions.

$$Q = \frac{2}{3} C_d L \sqrt{2g} H_t^{3/2} \tag{4}$$

In Eq. (4), Q is the weir discharge; C_d is a dimensionless discharge coefficient that varies with weir type, geometry, crest shape, and flow conditions; L is the weir crest length; g is the gravitational acceleration constant; and H_t is the free-flow (non-submerged) upstream total head relative to the weir crest elevation (see Fig. 4). H_t was used rather than the piezometric head (h) in an effort to better account for the effects of approach flow velocities. Upstream depth measurements were made 6.5P (approx. 1 m) upstream of the weir using a stilling well equipped with a point gage (±0.15 mm). H_t was then computed as h plus the velocity head at the measurement location ($H_t = h + V^2/2g$).

Due to multiple crest elevations for a single weir, particular attention must be given to the definition of h for a staged labyrinth. In this study, head-discharge data were collected for two different scenarios: (a) discharges isolated to the lower stage segments and (b) discharges where the entire weir crest was engaged. When flow was limited to the low stage, the upstream piezometric head for the low stage (h') was measured relative to the lower crest elevation and low stage weir height (P') with the total head for the low stage (H_t') computed as h' plus the velocity head (see Fig. 15a). When flow was conveyed over the entire labyrinth weir, h was measured relative to the high stage to compare the staged weirs to a traditional labyrinth with a single crest elevation (see Fig. 15b).

Low Stage-Isolated Discharge

Multiple head-discharge data points were collected for Models 1a, 1b, and 2-5 when flow was isolated to the low stage (see Appendix B). These data were compared with $Q_{predicted}$ values determined by Eq. (4) using: experimentally determined H_t' values, non-staged quarter-round crest labyrinth weir C_d data (collected from Model 6), and l_{stage} for the characteristic weir length. For models 1a and 1b, broad crested weir C_d values (Johnson 2000) were applied. The predictive error (i.e., $Q_{predicted}/Q_{actual}$) is plotted in Fig. 16 vs. H_t'/P' (dimensionless headwater ratio relative to the low stage crest elevation).

As seen in Fig. 16, the predictive error was as large as 20%, with the error magnitude generally increasing with increasing H_t'/P'. For the majority of the models tested (Models 1a, 1b, 3, and 5), $Q_{predicted}$ was larger than Q_{actual} for all values of H_t'/P'. Models 2 and 4 showed the opposite trend at values of $H_t'/P' > 0.13$. This indicates that the discharge of the lower stage is location-dependent. Applying a one-dimensional weir equation, such as Eq. (4), will likely produce some error while approximating discharge

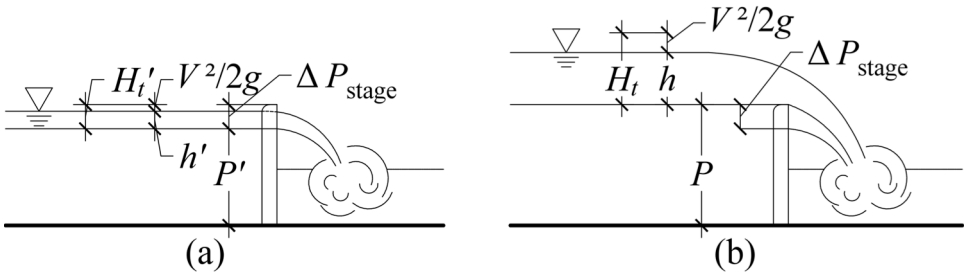

Fig. 15. Illustration of hydraulic parameters associated with (a) weir flow isolated to the low stage and (b) over the entire weir

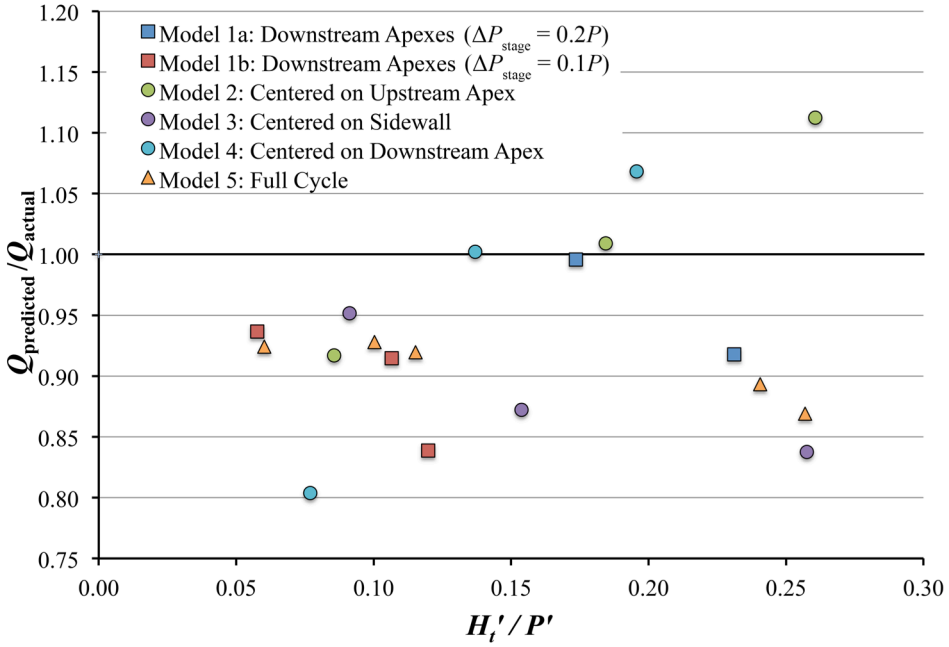

Fig. 16. $Q_{predicted}/Q_{actual}$ vs. H_t/P data ($Q_{predicted}$ calculated using the superposition method)

through the lower stage because labyrinth weirs are complex three-dimensional structures.

Staged Labyrinth Weir Discharge

When the entire labyrinth weir crest was engaged (flow passing over both stages), approximately 15 to 30 head-discharge data points were collected (for each staged labyrinth weir configuration) ranging from $0.1 < H_t/P < 2.0$, including high headwater ratios. C_d values for the entire spillway were computed for each measured flow condition and are presented in Fig. 17. An empirical curve-fit equation based upon the headwater ratio, H_t/P, is presented as Eq. (5) ($R^2 > 0.995$). This equation form was generated by curve fitting software and was specifically selected owing to its high correlation value for all experimental data sets and relative simplicity. Corresponding curve fit coefficients for Eq. (5), max and average error, and correlation values are presented in Table 4 and are recommended for the hydraulic design of geometrically similar staged labyrinth weirs for $0.1 < H_t/P < 2.0$.

$$C_d = a\left(b^{\frac{H_t}{P}}\right)\left(\frac{H_t}{P}\right)^c + d \tag{5}$$

As a result of applying the higher stage crest reference to the lower stage, the experimentally determined 'composite' C_d values of the entire spillway (Fig. 17) are greater at small H_t/P values than typical for C_d values for traditional labyrinth weirs (Model 5 returned values of $C_d > 1.0$). These C_d values can be higher or lower than

traditional labyrinth weir values depending on which stage is used as the reference crest elevation.

Staged Labyrinth Weir Discharge Capacity Estimation (Superposition Method)

To estimate staged labyrinth weir discharge capacities, the discharge for each labyrinth weir stage was calculated independently and summed. For the high stages, Eq. (4) was applied using H_t, the corresponding weir length (i.e., L - l_{stage}), and C_d values calculated using Eq. (5) and data from Model 6 (traditional labyrinth weir). For Models 1a and 1b, Eq. (4) was applied to the low stage using H_t', l_{stage}, and traditional flat-top weir C_d values (Johnson 2000) – the notches were limited to the downstream apexes and approximated as suppressed flat-top weirs with a converging approach flow channel. The low-stage discharges for models 2 through 5 were estimated as independent labyrinth weir elements and as contracted weir segments with $L = l_{stage}$ and $H_t = H_t'$. When considered to behave similar to contracted weirs, Eq. (6) (Haestad 2002) was selected as the head-discharge relationship, $C = 1.84$ (SI units). When judged to behave as a

Table 4. Coefficients for Eq. (5)

Model (#)	Location of Low Stage	Coefficients for Eq. (5)				R^2	Avg. Error	Max Error
		a	*b*	*c*	*d*			
1a	Downstream Apexes ($\Delta P_{stage} = 0.2P$)	0.9058	0.0976	0.3232	0.2407	0.9992	0.61 %	1.97 %
1b	Downstream Apexes ($\Delta P_{stage} = 0.1P$)	1.0264	0.0907	0.4290	0.2398	0.9983	0.66 %	1.82 %
2	Centered on Upstream Apex	0.6312	0.1701	0.0819	0.2309	0.9984	0.66 %	1.92 %
3	Centered on Sidewall	0.5427	0.1986	-0.0499	0.2306	0.9991	0.74 %	1.34 %
4	Centered on Downstream Apex	0.5641	0.2084	0.0107	0.2227	0.9951	1.17 %	4.22 %
5	Full Cycle	0.2617	0.7997	-0.6117	0.1445	0.9983	1.66 %	2.88 %
6	Standard Labyrinth	1.3400	0.0616	0.5860	0.2489	0.9989	0.78 %	2.79 %

Note: ΔP_{stage} = depth of stage; P = weir height; a, b, c and d = empirical coefficients from Eq. (5).

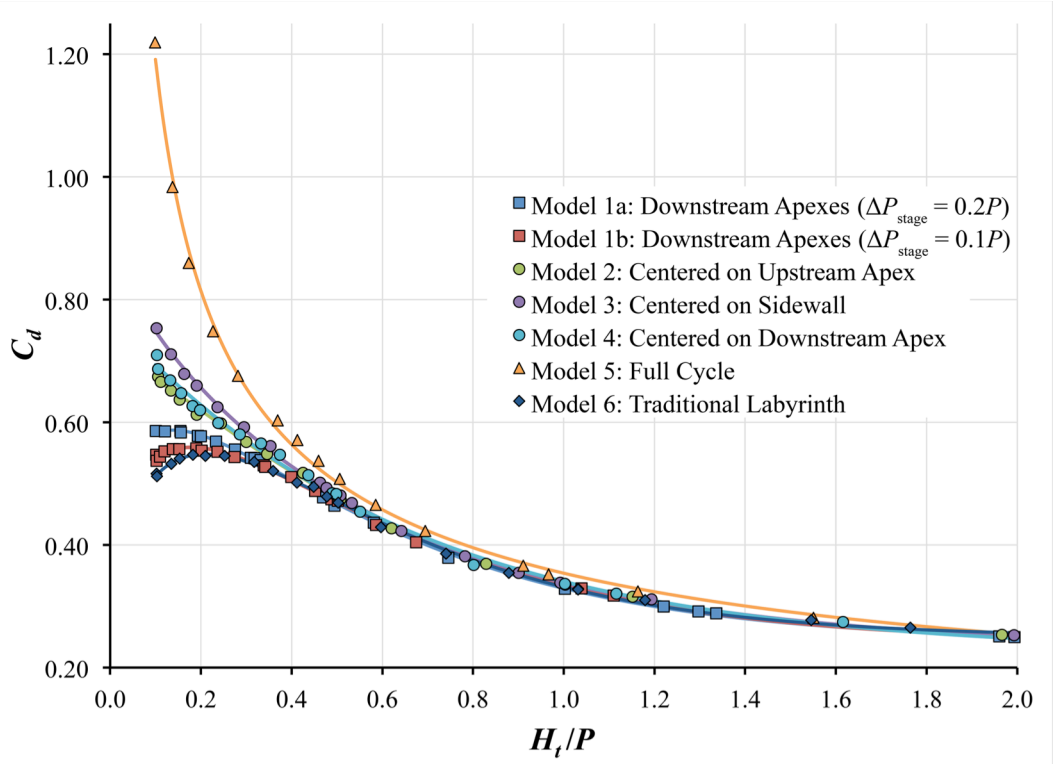

Fig. 17. C_d vs. H_t/P for discharges limited to the lower staged section(s)

traditional labyrinth weir, Eq. (4) was applied with C_d values corresponding to H_t'/P' calculated using Eq. (5).

$$Q = C(L - 0.1iH_t)H_t^{3/2}, \text{ where } i = \text{the \# of contractions} \quad (6)$$

The estimated Q for the staged labyrinth weir was estimated as the sum of all estimated stage Q values. While this method and appurtenant equations presently does not allow for an empirical adjustment to account for influences on approach flow conditions or energy loss associated with flow contraction/separation, it does represent a simple and practical design alternative in the absence of geometry-specific, staged labyrinth weir experimental head-discharge data. The accuracy of the superposition

method was juxtaposed with the experimental data sets developed in this study. The contracted weir assumption for the low stage [Eq. (3)] proved to be less accurate (approaching +10% when $H_t/P > 1.0$) than applying traditional labyrinth weir C_d and Eq. (4) for estimating Q. Hence, only the latter prediction results are discussed. $Q_{predicted}/Q_{actual}$ vs. H_t/P data for the staged labyrinth weirs investigated herein are presented in Fig. 18. Note that the staged labyrinth data are presented in terms of H_t to facilitate a graphical presentation of the results, even though H_t' was used in the low-stage calculations.

For $H_t/P < 0.5$, the superposition method underestimated the staged labyrinth spillway discharge by up to 15%. For $H_t/P > 0.5$, the accuracy of the predicted Q using the superposition method for Models 3 and 4 was ±5%. Models 1a, 1b, and 2 were computed to be within ±6% for all H_t/P values tested. Models 3 (sidewall stage) and 5 (full-cycle low stage) had the most variability with estimate accuracy ranging from -15% to +3% and -13% to +4% respectfully. Table 5 summarizes the maximum superposition method error for each model over specified ranges of H_t/P.

Table 5. Maximum Superposition Error for Ranges of H_t/P

Model (#)	Location of Low Stage	$0.1<H_t/P<0.25$	$0.25<H_t/P<0.5$	$0.5<H_t/P<1.5$	$1.5<H_t/P<2.0$	Avg. Error
1a	Downstream Apexes ($\Delta P_{stage} = 0.2P$)	-3.9%	3.1%	4.4%	5.5%	3.7%
1b	Downstream Apexes ($\Delta P_{stage} = 0.1P$)	1.7%	1.7%	3.5%	5.3%	2.5%
2	Centered on Upstream Apex	5.6%	2.7%	1.5%	3.2%	1.4%
3	Centered on Sidewall	8.2%	3.6%	2.1%	4.4%	1.9%
4	Centered on Downstream Apex	14.7%	6.8%	1.6%	2.8%	2.2%
5	Full Cycle	12.2%	5.9%	4.5%	4.1%	3.1%

Note: ΔP_{stage} = depth of stage; P = weir height; H_t = total upstream head of weir relative to the normal weir crest elevation.

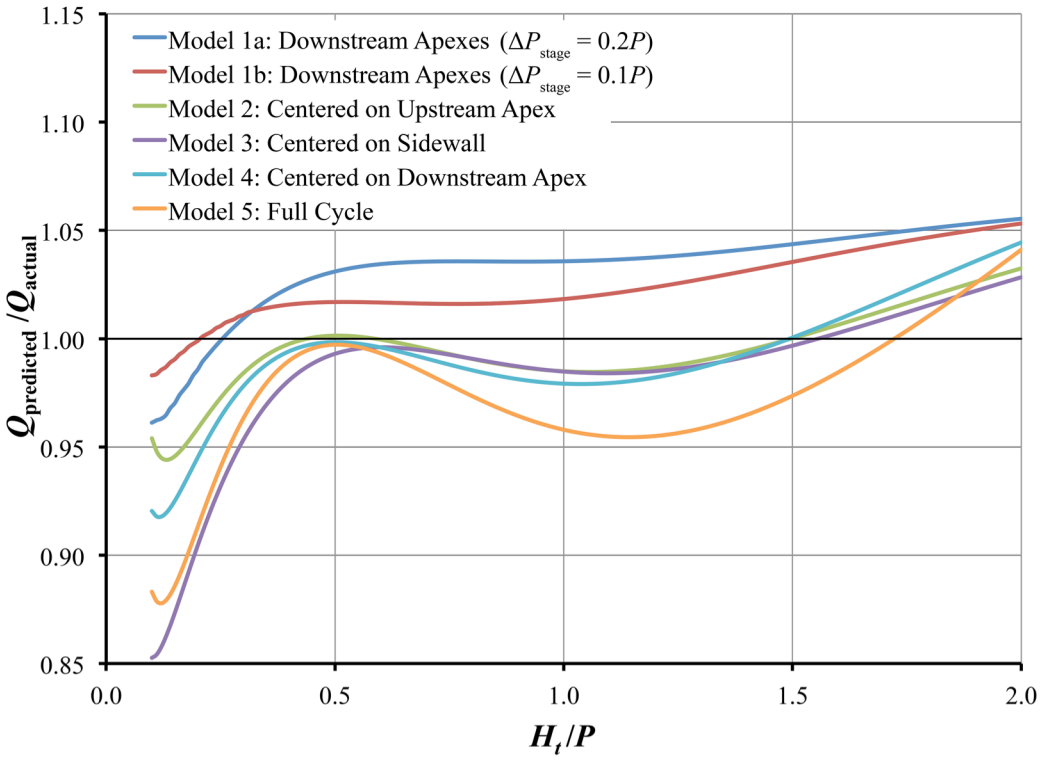

Fig. 18. Staged labyrinth weir $Q_{predicted}/Q_{actual}$ vs. H_t/P data ($Q_{predicted}$ calculated using the superposition method)

Influence of ΔP_{stage} at Labyrinth Apex (Models 1 and 1a) on Discharge

For Models 1a and 1b, ΔP_{stage} equaled $0.2P$ and $0.1P$, respectively. While Model 1b did produce higher discharges than the traditional labyrinth at low levels of H_t/P (see Fig. 17), the difference in flow efficiency became negligible for $H_t/P > 0.3$. Model 1a produced C_d values similar to that of a normal labyrinth when $H_t/P > 0.4$ (see Fig. 17).

Flow Distribution along Crest

A significant decrease in the water surface profile (drawdown effect) was observed within the high-stage labyrinth cycles of Model 5, adjacent to the low-stage cycle (middle cycle). It was clearly observed that, relative to the left and right distal cycles, less

flow was conveyed over the adjacent high-stage cycles. Based upon experimental observations, flow redistribution between cycles was likely present for all tested models and gives explanation for differences between experimental and predicted head-discharge data. To clarify, a non-uniform flow distribution would produce spatially varied C_d values that are unique to staged labyrinth weirs. Because Eqs. (4), (5), and (6) assume a constant value of H_t and experimental C_d values were structure and not stage-specific, some level of error should be anticipated when applying to labyrinth weirs with multiple engaged stages.

Flow Separation

Flow separation regions developed when the approaching flow encountered the crest elevation offset at the staged weir segment transitions (abrupt boundary change). The diverging and subsequent re-converging flow caused an increase in local turbulence and form loss (see Fig. 19). The staged segment transitions effectively reduced l_{stage} and consequently hydraulic efficiency. Flow separation was observed for all staged labyrinth

Fig. 19. Flow separation at stage transition of sidewall (Model 4)

weir geometries tested for flows isolated to the low stage and for flows passing over both stages. As Q (and H_t/P) increased, the flow separation was reduced at the stage transitions. Treating the stage segment transitions could increase hydraulic efficiency. For example, rounding the vertical corners would likely decrease flow separation. However, hydraulic efficiency should be balanced with spillway effectiveness, as such treatments would increase prototype construction costs for what might be a minimal hydraulic gain.

Downstream Effects

The staged labyrinth weir geometries tested herein were observed to produce non-uniform and asymmetrical flow patterns within the downstream labyrinth cycles and in the channel immediately downstream. Flow imbalance across the staged segment(s) resulted in additional splash, spray, and standing waves as flows interacted and collided downstream. The observed downstream flow behaviors may produce conditions (e.g., wave action) not accounted for in general design guidelines for downstream channels and chutes or common energy dissipation structures.

Conclusions

The goal of this study was to document and evaluate, under controlled laboratory conditions, the flow characteristics and hydraulic performance of various staged labyrinth weir geometries. This study also assessed the accuracy of a simple head-discharge prediction method based upon the principle of superposition. The computed $Q_{\text{predicted}}$ values were generally within ±5% of the experimentally determined Q_{actual}, with maximum errors of 15%. The predictive accuracy was determined to be a function of

H_t/P, ΔP_{stage}, l_{stage}, and the low stage location. Although only a single sidewall angle was tested in this study, labyrinth weir literature has documented that discharge is also a function of additional labyrinth geometric parameters, of which α would be a significant parameter in C_d and staged labyrinth weir Q estimations.

The documented hydraulic characteristics and flow behaviors observed in the laboratory provide new insights and are presumed to generally apply to staged labyrinth weirs. Nevertheless, the experimental results presented herein are limited to the staged labyrinth weir geometries tested. The results are recommended for estimating head-discharge relationships and outflow hydrographs for geometrically similar staged labyrinth weirs and as a first-order approximation for staged labyrinth weirs of different cycle geometries. Please note that a physical model study is recommended to confirm hydraulic characteristics of a staged labyrinth weir. Future studies of different nonlinear weir designs will further expand our understanding of these complex hydraulic structures.

CHAPTER IV

MODIFYING THE DOWNSTREAM HYDROGRAPH WITH STAGED LABYRINTH WEIRS[§]

Abstract

Labyrinth and piano key weirs are hydraulically more efficient than linear weirs of the same width. As the spillway discharge efficiency increases, the required reservoir detention volume reserved for flood routing reduces and the maximum base-flow operating reservoir pool elevation can subsequently be increased (additional water storage). Increased spillway discharge efficiency also causes the reservoir outflow hydrograph to compress temporally and the peak outflow discharge to increase, potentially increasing downstream flooding impacts. The influence of linear, labyrinth, and staged labyrinth weir (i.e., cycles with different crest elevations) head-discharge characteristics on the outflow hydrograph behavior was evaluated by numerically routing various flood discharges through a fictitious reservoir; peak outflow discharges, the maximum water surface elevation, and the required detention volumes were quantified for each weir alternative. In addition to the benefit of isolating base flows to a subset of the labyrinth weir, the staged labyrinth weir proved to be an effective alternative for modifying (decreasing) the spillway discharge efficiency to limit downstream flooding impact for higher return period storm events.

[§] Coauthored by Blake P. Tullis

Introduction

Labyrinth Weirs

Dams are critical infrastructure components that provide water supply (municipal, agricultural, industrial), flood control, hydropower, and recreation. Changes in land use, aging infrastructure, and higher peak flow predictions for extreme flood events often require upgrading existing spillways to increase discharge capacity. Replacing a linear weir with a nonlinear weir (e.g., replacing an ogee-crested weir with a labyrinth weir in many cases) is a common method for increasing spillway discharge capacity and improving dam safety.

The geometry of a labyrinth weir can significantly increase the weir crest length within a fixed-width channel relative to a linear weir. Because a weir's discharge is proportional to its length, this can increase discharge capacity by 3 to 4 times (Tullis et al. 1995). Common geometric variables for labyrinth weir design are shown in Fig. 20, where P is the weir height, α is the sidewall angle, w is the cycle width, W is the channel width, and l_c is the sidewall centerline length. Because of their hydraulic performance, labyrinth weirs have been of interest to practitioners and researchers for many years. A

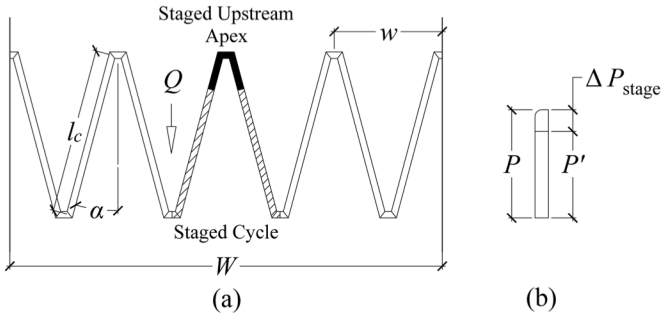

Fig. 20. Geometric variables of labyrinth and staged labyrinth weirs in (a) plan and (b) elevation view

partial list of publications related to the design and hydraulic performance of traditional (non-staged) labyrinth weirs: Tullis et al. (1995), Magalhães and Lorena (1989), Falvey (2003), Tullis et al. (2007), and Crookston and Tullis (2012a, b; 2013a, b); Chapter III of this text reports hydraulic performance data for specific staged labyrinth weir geometries. The preceding publications primarily focus on the design and hydraulic capacity of labyrinth weirs, with little discussion regarding potential downstream flooding impact.

In addition to passing the more extreme flood events [e.g., the Probable Maximum Flood (PMF), 500-year flood, etc.], an upgraded hydraulically more efficient spillway design may also be required to limit spillway discharges to pre-development peak outflows for the more frequent return-period storm events to satisfy downstream flood-control performance criteria (Campbell and Binder 1991; Paxson and Binder 2009). Different spillway types installed in parallel (e.g., gated and ungated spillways) can be an effective means of meeting a prescribed outflow hydrograph requirement during flood routing events. Because of maintenance requirements and the requirement for active control (i.e., operator present), gated spillways may no be suitable for some parallel spillway control structure applications. An alternative passive-flow-control parallel flow control structure solution could be a labyrinth weir that incorporates weir segments with different elevations (i.e., staged labyrinth weir).

Staged Labyrinth Spillways

A variety of staged weir spillway types, including ogee crest and labyrinth weirs as shown in Fig. 21, have featured parallel flow control structures (i.e., gated/non-gated and/or varied crest elevations). Staged labyrinth weirs are essentially parallel labyrinth

Fig. 21. Photos of staged ogee-crested weir (Tom Miller Dam, TX) and staged labyrinth weir (Lake Townsend, NC). Courtesy of: Michael Johnson and Brian Crookston

weirs. Geometric variables specific to staged labyrinth weirs are presented in Fig. 20, where P is the height of the high stage, P' is the height of the low stage, and ΔP_{stage} is the difference between P and P'.

When designing a staged labyrinth weir, the lower stage weir segment crest elevation is set at the normal pool elevation and conveys base flows and runoff from relatively frequent storm events (e.g., the 500-year, 100-year, etc.); for reservoir applications without a normal pool elevation, the lower stage crest elevation would be set at the maximum allowable base flow reservoir elevation. The higher stage weir segment is engaged and provides additional discharge capacity during more extreme flood events. In addition to matching higher frequency return period flood discharge requirements, confining base flow and smaller storm event outflows to lower staged sections can also be beneficial by limiting the extent of potential biological growth (e.g., algae) on the weir structure; floating debris collection and removal for base flow conditions is also confined to the lower staged portion of the spillway.

Labyrinth weirs are often used to increase spillway capacity, which limits potential upstream flooding and improves dam safety. Increasing the discharge efficiency of the flow control structure can have significant impact on downstream flood routing. In addition to improving dam safety, limiting the downstream flooding effects, in some cases, may represent a significant spillway performance criteria associated with designing a spillway flow control structure. As the discharge efficiency of the outlet flow-control structure increases, the required detention volume required in the reservoir for flood routing decreases and the peak outflow increases. This study uses flood-routing examples to demonstrate the influence of different spillway weir types on the reservoir and outflow hydrograph behavior. While the example presented herein is fictitious, similar analysis can be used to develop staged labyrinth weir designs that balance reservoir flood routing and outflow hydrograph performance requirements.

Using published head-discharge data for staged labyrinth weirs, non-staged labyrinth weirs (see Chapter III), and ogee crest weirs (USBR 1987), three different flood hydrographs were routed through a fictitious reservoir featuring four different spillway flow control structure alternatives (e.g., ogee-crested linear weir, a labyrinth weir, and two different staged labyrinth weirs to evaluate their influence both upstream and down.

Numerical Model Setup

Reservoir and weir characteristics

A 1,500 m square reservoir with a trapezoidal cross-section, a 16.1 m wide spillway and a normal pool elevation of 200 m was used as a model to route the inflow hydrographs. Three sides of the reservoir sloped at 1:4 (vertical:horizontal) to increase

the area of the reservoir with increasing water depth; the downstream reservoir boundary, which contained the spillway, was vertical. The simplified reservoir shape was selected to maintain simplicity in the model.

All labyrinth weirs modeled were geometrically similar to the laboratory-scale models tested by Dabling et al. (2013), but scaled to a prototype $P = 4$ m. The ogee-crested weir maintained the same channel width, weir height, and crest elevation. The crest coefficient for the ogee-crested weir was consistent with USBR guidelines (USBR 1987). The two staged labyrinth weirs included a full-cycle low stage (1-cycle) and upstream-apex low stage (US apex) that was equal to one half the sidewall centerline length (see Fig. 20). For both models $\Delta P_{stage} = 0.2P$ (0.8 m).

Flood Routing Analysis

Three inflow storm hydrographs were routed through the model reservoir using the storage indication method (Haestad 2002) with a time step of 0.1 hours. The storage (S'), inflow (I), outflow (O), and reservoir elevation at each time step were calculated using Eq. (1); the variable subscripts "n" and "n+1" represent the values for the current and subsequent time step. Each model inflow hydrograph had a 24-hour duration; the peak discharges were 300 m^3/s, 75 m^3/s, and 37.5 m^3/s respectively, which were assumed representative of a PMF, 500-year, and 100-year return-period flood events and are referenced in the text and figures accordingly. The initial water level in the reservoir and crest elevations for the ogee and the non-staged labyrinth weir were set at elevation 200 m. For the staged labyrinth weirs, the lower stage was placed at elevation

200 m and the high stage placed at elevation 200.8 m, establishing a common normal pool elevation for each scenario.

$$\left(\frac{2S'_{n+1}}{\Delta t}+O_{n+1}\right)=\left(\frac{2S'_{n}}{\Delta t}-O_{n}\right)+\left(I_{n}+I_{n+1}\right) \tag{7}$$

Experimental Results and Discussion

Outflow Hydrograph

Using Eq. (7), reservoir outflow hydrographs were obtained for the ogee crested, labyrinth, and staged labyrinth weirs for each of the three inflow hydrographs described (see Figs. 22-24). The reservoir storage required to pass the inflow hydrograph for each of the four weirs examined was calculated by summing the differences between inflow and outflow values until the time of maximum reservoir discharge. With increased spillway efficiency (higher discharge for a given reservoir elevation), the outflow hydrograph for the labyrinth weir occurred over a compressed timeframe, and the maximum outflow peak increased as expected. This can potentially create adverse flooding effects downstream if the downstream channel has insufficient carrying capacity. The relative changes in peak reservoir outflow discharge and storage volume requirements for the staged and non-staged labyrinth weirs, relative to the ogee crest weir performance, are summarized in Table 6 for the three inflow hydrograph examples.

Reservoir and Outflow Hydrograph Response

According to the data presented in Table 6, the labyrinth weir is hydraulically more efficient than the ogee crest weir (as expected) for all three inflow hydrographs; the

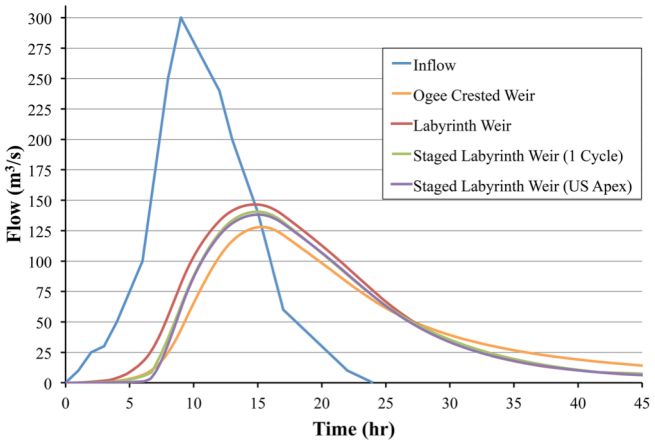

Fig. 22. Spillway-specific outflow hydrographs for inflow hydrograph-PMF (peak inflow = 300 m^3/s)

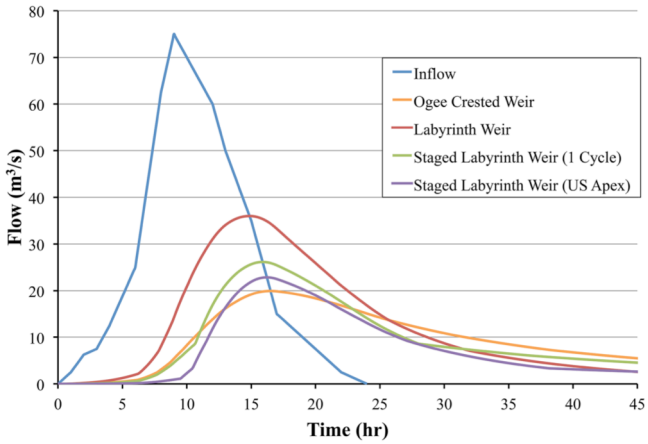

Fig. 23. Spillway-specific outflow hydrographs for inflow hydrograph-500 (peak inflow = 75 m^3/s)

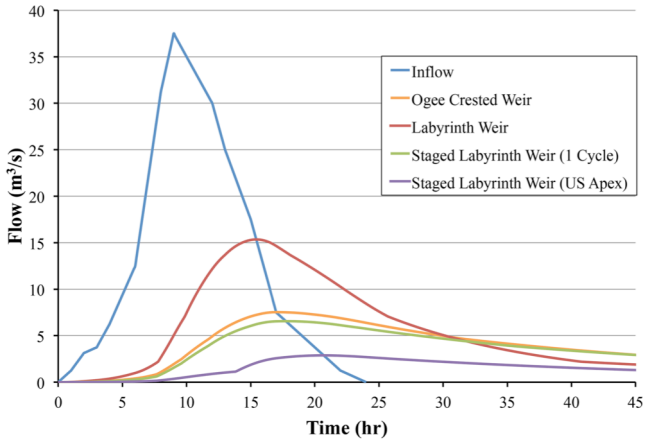

Fig. 24. Spillway-specific outflow hydrographs for inflow hydrograph-100 (peak inflow = 37.5 m^3/s)

Table 6. Discharge and Storage Data

Model	Hydrograph (#)	Relative Change in Peak Outflow	Relative Change in Flood-Routing Reservoir Storage	Relative Change in Maximum Reservoir Elevation
Labyrinth Weir	PMF	14.4%	-16.8%	-16.1%
	500	80.9%	-24.9%	-25.0%
	100	105.3%	-21.3%	-22.0%
Full-Cycle Staged Labyrinth Weir	PMF	9.7%	-8.4%	-8.3%
	500	31.2%	-4.4%	-3.9%
	100	-12.0%	3.0%	2.4%
US Apex Staged Labyrinth Weir	PMF	7.9%	-6.5%	-6.2%
	500	15.1%	3.2%	2.6%
	100	-61.3%	17.6%	17.1%

increase in discharge efficiency is considerably higher for the higher return period storms [e.g., Hydrograph-100 (105.3%), Hydrograph-500 (80.9%)] than for the PMF (14.4%)]. If the ogee crest and labyrinth weir spillways represented pre- and post-rehabilitation spillway configurations respectively, the labyrinth weir in this example would be unacceptable if the goal of the spillway upgrade was to increase discharged capacity for extreme events (e.g., PMF) while maintaining the downstream flooding risk at or near pre-upgrade conditions for higher frequency flood events. The staged labyrinth weir examples also increased the PMF [1-Cycle (9.7%), US Apex (7.9%)] and Hydrograph-500 [1-Cycle (31.2%), US Apex (15.1%)] discharge capacities relative to the ogee crest spillway. For the Hydrograph-100 conditions, however, the discharge capacities of the 1-Cycle and the US Apex staged labyrinth weirs were less efficient (-12% and -61.3%, respectively) than the ogee crest weir.

By calculating the change in reservoir storage, the upstream water elevations for the four spillway configurations were obtained and plotted vs. time for the three hydrographs in Figs. 25-27. The PMF performance of the staged labyrinth weir

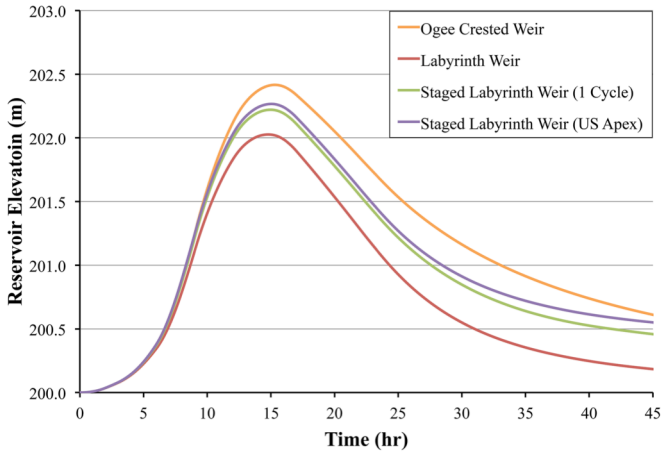

Fig. 25. Water elevation for hydrograph-PMF (peak inflow = 300 m^3/s)

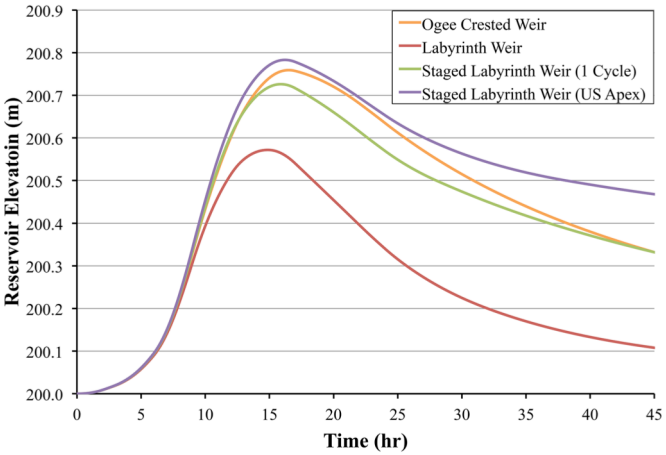

Fig. 26. Water elevation for hydrograph-500 (peak inflow = 75 m^3/s)

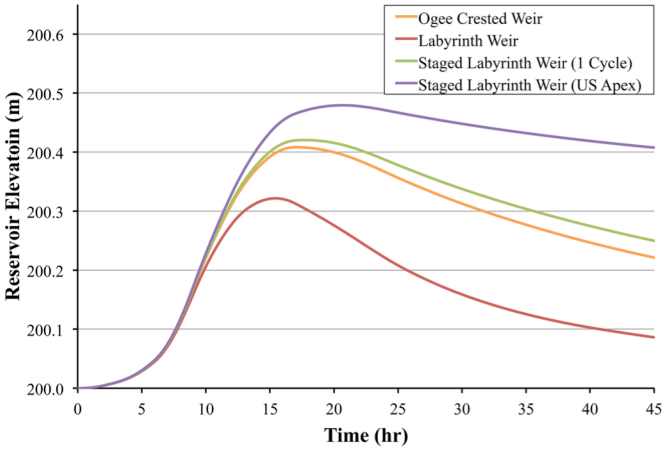

Fig. 27. Water elevation for hydrograph-100 (peak inflow = 37.5 m^3/s)

geometries, which fall between the more efficient labyrinth weir and the less efficient ogee crest weir, are nearly identical (see Figs. 22 and 25). As the flood return-period frequency increases, the behavior of the two staged-labyrinth weir geometries began to vary significantly from one another. Relative to the ogee crest weir, the required reservoir flood-routing detention volume for the Hydrograph-100 (see Table 6) increased by 3% for the 1-Cycle staged labyrinth weir; the US Apex configuration required a 17.6% increase in detention storage for the same flood event.

Figs. 24 and 27 illustrate similar trends with the maximum reservoir water surface elevation associated with routing the Hydrograph-100 flood event. Assuming no restrictions on detention volume use for reservoir flood routing, provided that the minimum reservoir free board requirement is not violated, the increases in reservoir detention volume use created by the decreased spillway discharge capacity for higher-frequency return-period flood events may not necessarily be a negative outcome; the potential for downstream flooding is actually reduced for the higher-frequency return period flood event relative to the ogee crest weir while the discharge capacity for the more extreme flood events increases (improved dam safety). Another potential side benefit of staged labyrinth weirs is that base flows and smaller flood events can be confined solely to the lower labyrinth weir stages, which could reduce maintenance costs. As mentioned previously, the taller labyrinth stage and corresponding downstream apron will remain dry for lower discharges (less potential for biological growth on wet surfaces) and any floating debris that may collect during low-flow events will be limited to the lower stage weir sections and more easily removed when required.

For cases where minimizing downstream flood risk is not of principal concern, using a labyrinth weir as the spillway flow control structure could prove beneficial. The labyrinth weir's high discharge efficiency means that less reservoir detention volume in the reservoir must be set aside for flood routing. While still maintaining the required minimum freeboard in the reservoir, the weir crest elevation can be raised above that of an ogee crest (or other hydraulically less efficient linear weir design) increasing both the normal pool reservoir storage volume and elevation without negatively impacting dam safety.

The sizes of the reservoir and spillway weir alternatives used in this discussion were arbitrarily selected and are not suggested as optimal solutions. It's important to note, however, that as the size of the reservoir decreases, the overall influence of the specific spillway head-discharge characteristics on the reservoir flood-routing detention response diminishes. The ability to reduce downstream flooding impact for higher-frequency return period flood events through prudent spillway flow control structure design diminishes as reservoir volume decreases.

Conclusions

Labyrinth weirs can decrease the maximum reservoir water elevation required to pass a flood event relative to a linear ogee crest weir. A staged labyrinth weir can decrease the required water level to a lesser extent, while providing the maintenance benefits of confining base flows and smaller flood events to a subset of the spillway width and decreasing the peak reservoir outflows during a large storm event. Using published labyrinth and staged labyrinth weir discharge data, a theoretical model of a

reservoir and inflow hydrograph was created, and a comparison of the downstream hydrograph, using the storage indication method for four weir configurations (ogee-crested spillway, labyrinth spillway, and two staged labyrinth spillways) was presented.

The sizes of the reservoir and spillway weir alternatives used in this discussion were arbitrarily selected and are not suggested as optimal solutions. The data presented are specific to the model reservoir, weirs, and inflow hydrograph evaluated, but they illustrate the potential effects of discharge efficiency and flood routing, which should always be considered when designing a spillway rehabilitation project and evaluating its potential for downstream flooding. Some key findings of this study include:

- Labyrinth weirs produce significantly larger peak outflows than less efficient spillways, increasing the potential for downstream flooding.
- Staged labyrinth weirs are also effective at decreasing the detention volume required to pass extreme flood events, while maintaining peak outflows that are approximately equal or less than the capacity of linear weir spillways (e.g. ogee crest in this example) for higher-frequency return period storm events.
- The overall influence of the spillway head-discharge characteristics on the reservoir flood-routing detention response diminishes as the reservoir size decreases.

Staged labyrinth weirs are not useful in every situation, but the design can be beneficial if additional spillway capacity is required for extreme events while minimizing downstream flooding potential for smaller flood events. It is important to consider that in

some cases downstream flooding may be necessary to safely pass larger flood events without dam failure. The ratio of staged weir lengths and heights as well as the overall weir length should be designed for site-specific conditions (e.g., inflow hydrology, downstream flow restrictions, available reservoir flood routing detention volume, etc.).

CHAPTER V

LABYRINTH WEIR HYDRAULICS WITH ANGLED APPROACH FLOW**

Abstract

The current design methods and research have primarily investigated the hydraulic characteristics of labyrinth weirs when the approach flow is perpendicular to the weir axis. In some cases, a perpendicular approach flow and weir axis alignment may not be possible. The head-discharge characteristics of a 4-cycle, 15° labyrinth weir with a channelized approach flow were evaluated with three different approach flow angles (0°, 15°, and 45°) using laboratory-scale physical models. While the data presented are specific to the geometry of weir and channel tested, it provides a general indication of discharge efficiency variation with as a function of approach flow angle. The experimental data were also compared with the head-discharge characteristics of prototype labyrinth weir model study that featured significant approach flow angles. For approach flow angles less than 15°, no measurable loss in discharge efficiency occurred, relative an approach flow angle of 0°. The discharge efficiency reduced by as much as 11% for the 45° approach flow angle case. Flow instability was observed downstream of the weir, producing unique flow patterns in the labyrinth cycles and on the spillway apron.

** Coauthored by Blake P. Tullis

Introduction

Labyrinth Weirs

Dams are a critical infrastructure component throughout the world, providing water supply (municipal, agricultural, industrial), flood control, hydropower, and recreation. Changes in surrounding land use, aging structural elements, and updated peak flow predictions for flood events often require dam rehabilitation. Linear weirs incorporated within a dam spillway can be replaced with nonlinear weirs (i.e. a labyrinth weir) to increase spillway discharge capacity without increasing the existing spillway channel width.

A labyrinth weir utilizes a folded geometry to increase the allowable weir crest length within a given channel width; the additional crest length can increase discharge capacity by 3 to 4 times (Tullis et al. 1995) over a linear weir. Geometric variables for labyrinth weir design are shown in Fig. 28, where P is the weir height, α is the sidewall angle, A is the apex width, w is the cycle width, W is the channel width, and l_c is the sidewall centerline length. Labyrinth weirs have been of interest to practitioners and researchers for many years, with notable design publications by Hay and Taylor (1970), Tullis et al. (1995), Falvey (2003), Crookston (2010), and Crookston and Tullis (2012a, b; 2013a, b).

Discharge characteristics of labyrinth weirs have been investigated for in-channel and reservoir applications, but most studies have limited the approach flow angle (β) perpendicular to the weir ($\beta = 0°$). Amanian (1987) conducted a few tests with $\beta = 0°$, 30° and 45° for a labyrinth weir ($\alpha = 24.5°$) in a channelized approach (no abutments) and found that increasing β resulted in a decrease in discharge efficiency, as measured by the discharge coefficient (C_d). The model tested was not consistent with current design recommendations, and was undersized. Tullis et al. (1995) recommended a limit of $\beta < 15°$ when applying their design method that was based on $\beta = 0°$ data.

While $\beta = 0°$ represents the more ideal labyrinth weir approach flow configuration, there may be situations when a perpendicular approach flow may not be feasible due to site specific constraints. As an example, the spillway on an existing dam in Texas (USA), which is being upgraded from a broad-crested to a labyrinth weir, features a long, shallow approach channel that runs parallel to the dam embankment. The spillway sits on bedrock and economic constraints required that the labyrinth weir be oriented parallel to the embankment, creating a significant approach flow angle. (see Fig. 29).

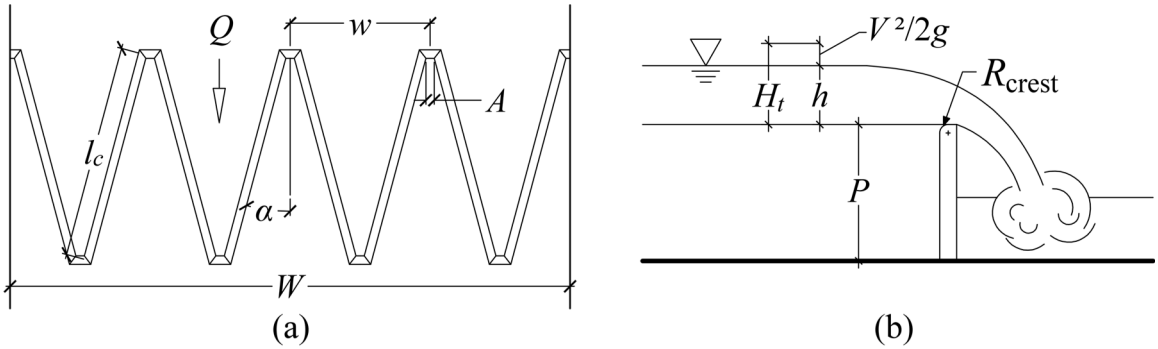

Fig. 28. Geometric design and discharge parameters of labyrinth weirs

The goal of the current study was to quantify the efficiency decrease of labyrinth weirs as β is increased, using a labyrinth weir consistent with current design methods. There was also a desire for accurate angled approach flow discharge data from a weir placed with reservoir contractions, as this is often the design that would be used in practice. Three approach flow angles were tested ($\beta = 0°$, 15°, and 45°), and data collected from a model of the prototype dam shown in Fig. 29 was used as a comparison.

Fig. 29. Overhead view spillway model study with a significant approach flow angle

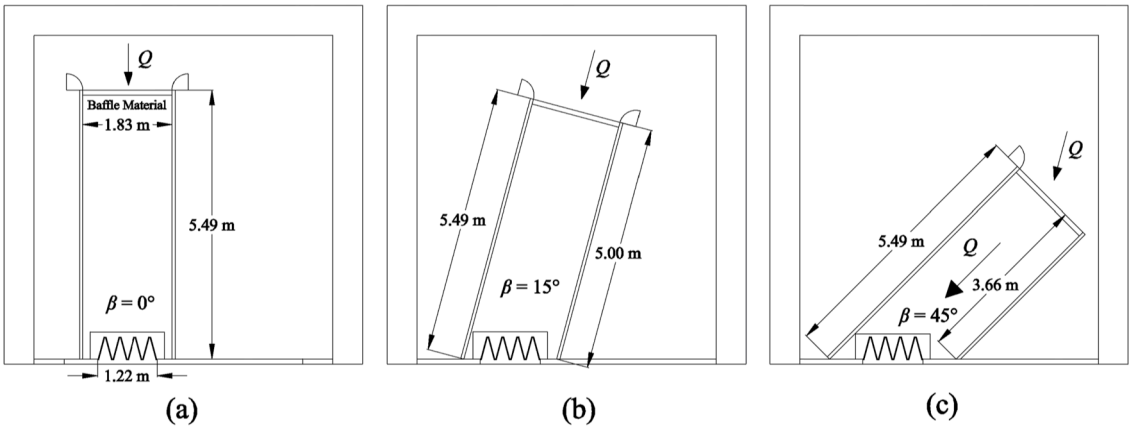

Fig. 30. Angled approach flow test configurations for (a) $\beta = 0°$, (b) $\beta = 15°$, and (c) $\beta = 45°$

Experimental Setup

Investigations were conducted at the Utah Water Research Laboratory (UWRL) at Utah State University. A 4-cycle ($N = 4$), $\alpha = 15°$ labyrinth weir ($P = 0.30$ m) with a quarter-round crest shape [$R_{crest} = 1/2$ the wall thickness (t_w)] and $W = 1.22$ m was installed at the end of a 1.83-meter approach channel that was placed inside head box (see Fig. 30). The wider approach flow channel, relative to W, was necessary to physically accommodate the $\beta = 45°$ while keeping the approach channel centerline aligned with the downstream middle apex and maintaining a constant approach channel width. This necessitated square-edged (each $0.37W$ long) abutment walls on both sides of the labyrinth weir, which resulted in contracting flow conditions near the distal ends of the labyrinth weir. Discharge (Q) was measured using a magnetic flow meter (±0.25% accuracy). The upstream piezometric head (h) was measured using a stilling well and point gauge (readable to ±0.15 mm) hydraulically connected to the approach channel sidewall approximately 2 meters upstream of the weir (see Appendix C).

Experimental Results

Head-discharge Performance

Eq. (8), a form of the standard weir equation (Henderson 1966), was selected to quantify the labyrinth weir head-discharge relationships; the corresponding discharge coefficients were used to characterize discharge efficiency for the various approach flow conditions.

$$Q = \frac{2}{3} C_d L \sqrt{2g} H_t^{3/2} \tag{8}$$

In Eq. (8), Q is the weir discharge; C_d is a dimensionless discharge coefficient that varies with the weir design and flow conditions; L is the weir centerline crest length; g is the gravitational acceleration constant; and H_t is the free-flow (non-submerged) upstream total head relative to the weir crest elevation (see Fig. 28). H_t was used rather than the piezometric head (h) in an effort to better account for the effects of approach flow velocities, and was calculated as h plus the velocity head at the measurement location ($H_t = h + V^2/2g$). C_d was then calculated and plotted against H_t/P in Fig. 31.

Perpendicular Approach Flow

Data for the $\beta = 0°$ configuration were compared with Crookston (2010) discharge coefficient data collected for a labyrinth weir geometrically identical to the weir tested in the current study. The Crookston (2010) weir was tested in a channel with a channel width equal to W (no flow abutment walls nor flow contraction edge effects). At low heads (H_t/P), the flow contraction effects in the current ($\beta = 0°$) study are small and there is relatively good agreement with the Crookston (2010) data. At higher heads (H_t/P), the flow contraction effects become more significant and labyrinth weir/approach channel configuration becomes less efficient relative to the no-abutment, channelized approach flow condition tested by Crookston (2010).

Angled Approach Flow

When the approach flow was angled to the Tullis et al. (1995) recommended limit of $\beta = 15°$, there was no measureable decrease in efficiency, relative to $\beta = 0°$ over the

Table 7. Trend Line Equation Coefficients [Eq. (9)]

β	Coefficients for Eq. (9)			
	A	*B*	*C*	*D*
0 - 15°	0.007845	-4.2961	0.4360	0.2799
45°	0.005432	-4.8180	0.4337	0.2550

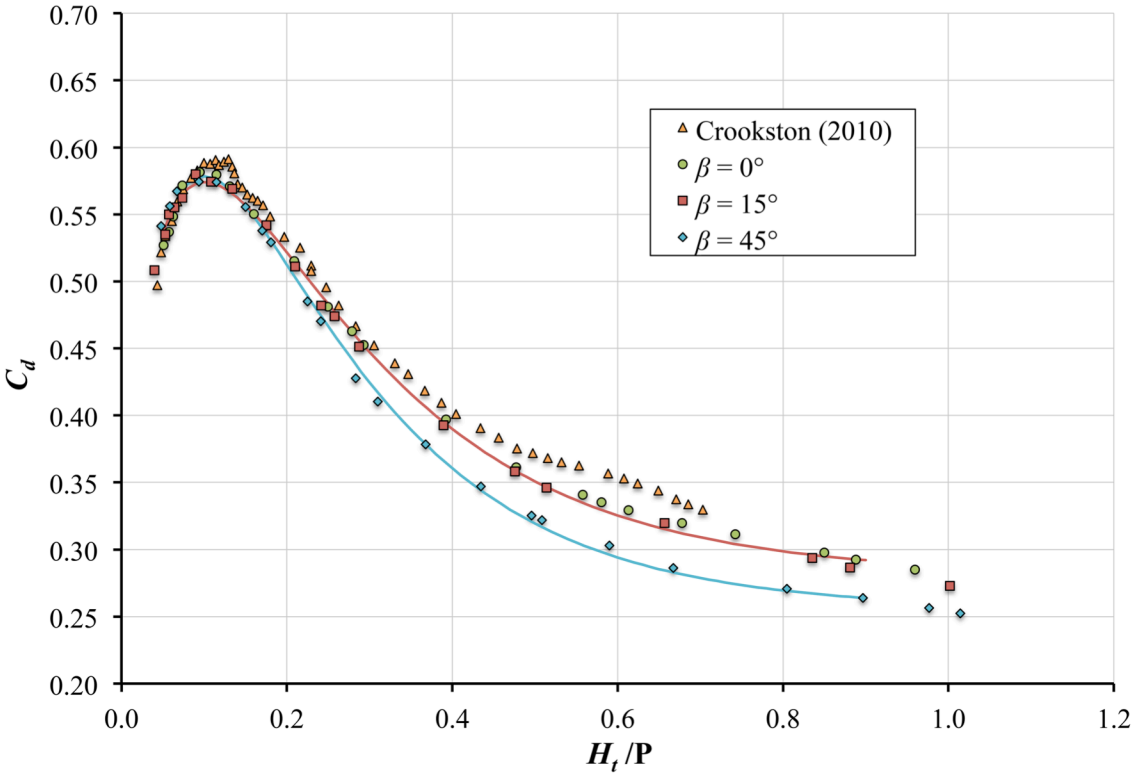

Fig. 31. Head-discharge data for tested physical models compared to Crookston (2010)

range of H_t/P tested as shown in Fig. 31. When the approach flow angle was more extreme (β = 45°), C_d decreased by as much as 10% at the higher H_t/P values.

For convenience, the trend line equations [Eq. (9)] were fit to the C_d data. This equation was chosen because of its high accuracy ($R^2 > 0.997$) and to be consistent with previous design labyrinth weir studies. The coefficients are presented in Table 7, and trend lines are graphed in Fig. 31.

$$C_d = A\left(\frac{H_t}{P}\right)^{\left[B\left(\frac{H_t}{P}\right)^C\right]} + D \tag{9}$$

The percent difference in C_d for $\beta = 45°$ and $\beta = 0°$ was calculated using the trend line equations and is plotted in Fig. 32. At low H_t/P values there is little impact on hydraulic efficiency with an angled approach flow as the relatively low approach flow velocity essentially replicates a reservoir approach flow boundary condition. As the upstream approach velocity and momentum increase with increasing H_t/P, the influence of the non-perpendicular approach channel becomes more significant. For the $\beta = 45°$ case, each labyrinth weir cycle features what could be described as the equivalent to a windward and leeward sidewall. The better alignment with the approach flow results in more discharge passing over windward sidewall than the leeward sidewall. Flow separation also occurs near the upstream apex, resulting in wakes or standing wave development on the leeward side.

The flow patterns in labyrinth weir outlet cycles is very three dimensional and turbulent. When the approach flow angle become extreme, the scale of the large turbulent

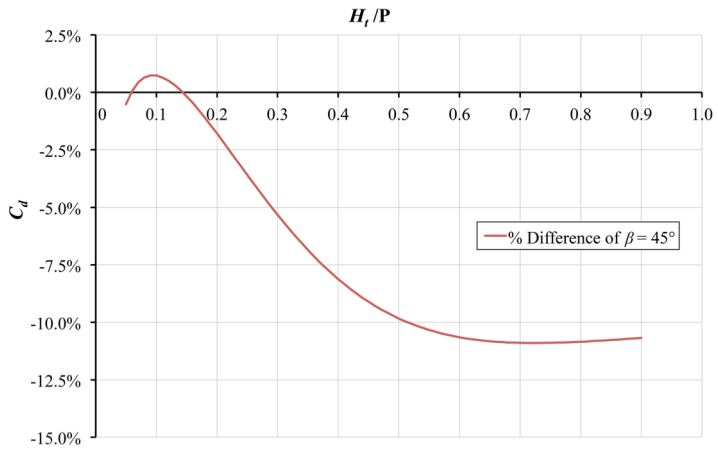

Fig. 32. %Difference of $\beta = 45°$ curve compared to perpendicular approach flow curve

flow patterns increases the nature of the flow characteristics changes; non-uniform approach flow relative to the labyrinth weir cycle alignment produces a more helical flow pattern in the labyrinth weir outlet cycles. When local submergence of the upstream apexes occurs, the momentum of the approach flow can carry it across the upstream end of an outlet cycle and into the adjacent cycles as it moves downstream (see Fig. 33). The nappe aeration characteristics also change with extreme approach flow angles, resulting in more spacial and temporal fluctuations.

Comparison with Prototype Model Study Data

The data collected are compared to the prototype model mentioned earlier. For the prototype structure, the spillway had to be constructed at the end of an earthen dam to allow for proper rock stability anchoring. This created a long approach channel, which required flow to curve significantly before reaching the spillway. The approach flow

Fig. 33. Flow conditions for $\beta = 45°$, showing imbalance at (a) $H_t/P = 0.5$ and (b) $H_t/P = 1.0$

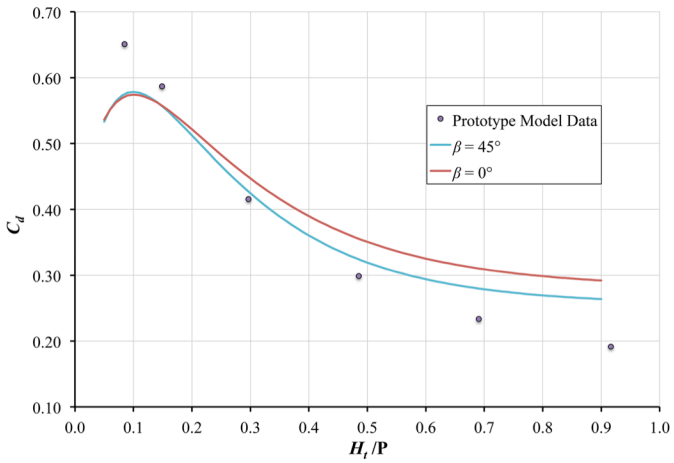

Fig. 34. Prototype model study data comparison

angles at the labyrinth varied across the channel from β = 60-70° on the left side to β = 0° on the right side of the weir.

The prototype model study C_d vs. H_t/P data with its non-uniform approach flow angle are compared to the results of the current study in Fig. 34. At low head levels, the prototype spillway is slightly more efficient due to the utilization of an ogee-style crest on the weir and rounded upstream and downstream apexes (Willmore 2004). However, as the discharge increases, the efficiency is greatly reduced because of the unconventional approach, and at high ends was as much 40% less efficient than a standard labyrinth with β = 0°.

Conclusions

The goal of this study was to investigate the potential decrease in efficiency of a labyrinth weir when used in conjunction with an angled approach flow. Three different approach flow angles were tested, including perpendicular to the weir (β = 0°), at the limit described by Tullis et al. (1995) (β = 15°), and at an extreme angle (β = 45°). The

results validated the $\beta = 15°$ guideline set by Tullis et al. (1995), showing that there was no measureable decrease in efficiency at this approach angle. However, as the angle was increased, the discharge coefficient C_d was decreased by as much as 11%. Prototype models of structures validate this analysis, and suggest that at higher levels of β, the increase in efficiency may be much greater.

Future work could include testing a broader range of β, possibly using computational fluid analysis to validate the approach angle limit suggested by Tullis et al. (1995).

CHAPTER VI

CONCLUSIONS

Nonlinear weirs are extremely useful structures. By folding the geometry of a weir, a significant increase in crest length can be designed without requiring an increase in channel width. If designed properly, using published literature and good engineering judgment, a nonlinear weir can decrease upstream flooding risk in both reservoirs and hydraulic channels.

This study investigated four subjects of nonlinear weir hydraulics, based on furthering current knowledge on both labyrinth and piano key weirs:

1. Discharge characteristics of piano key weirs with tailwater submergence
2. Discharge characteristics of staged (notched) labyrinth weirs
3. Modifying the outflow hydrograph of a reservoir using staged labyrinth weirs
4. Discharge efficiency of labyrinth weirs with an angled approach flow

The goal of each study was to increase understanding of the complex three-dimensional flows over nonlinear weirs, by applying simplified one- and two-dimensional hydraulics. Because of the infinite number of configurations for a nonlinear weir design, this simplified approach allows the results of each study to apply generally to many situations.

Piano Key Weir Submergence in Channel Applications

The purpose of this study was to characterize the submerged head-discharge characteristics for two configurations of weir and compare them with submerged labyrinth weir behavior. Relative to the sharp-crested linear and labyrinth weir dimensionless submerged-head relationships presented by Tullis et al. (2007) and to each other, the piano key weirs tested produced unique dimensionless submerged head characteristics that were discharge specific.

Although minor, both weirs tested were hydraulically more efficient (~6% maximum) than the labyrinth weir at relatively low levels of submergence. This effect is reversed at higher submergence levels. The hydraulic efficiency of the submerged standard piano key weir exceeded that of the modified piano key weir (with rounded upstream apexes and parapet walls). For both piano key weir configurations tested, as discharge was increased, the modular submergence range (maximum downstream water level where the upstream water level is not effected) also increased.

Staged Labyrinth Weir Hydraulics

The goal of this study was to document and evaluate, under controlled laboratory conditions, the flow characteristics and hydraulic performance of multiple configurations of staged labyrinth weirs. This study also assessed the accuracy of a simple head-discharge prediction method based upon the principle of superposition. The computed $Q_{predicted}$ values were generally within ±5% of the experimentally determined Q_{actual}, with maximum errors of 15%.

The documented hydraulic characteristics and flow behaviors observed in the laboratory provide new insights and are presumed to generally apply to staged labyrinth weirs. Nevertheless, the experimental results presented herein are limited to the staged labyrinth weir geometries tested. Superposition was determined to be a good first-order approximation for a staged labyrinth weir.

Modifying the Downstream Hydrograph with Staged Labyrinth Weirs

Labyrinth weirs can decrease the maximum reservoir water elevation required to pass a flood event relative to a linear ogee crest weir. A staged labyrinth weir can decrease the required water level to a lesser extent, while providing the maintenance benefits of confining base flows and smaller flood events to a subset of the spillway width and decreasing the peak reservoir outflows during a large storm event. Using the storage indication method for four weir configurations (ogee-crested spillway, labyrinth spillway, and two staged labyrinth spillways), a theoretical numerical model of a reservoir and inflow hydrograph was created, and a comparison of the downstream hydrograph was performed.

The results of this comparison indicate that labyrinth weirs produce significantly larger peak outflows than a less efficient spillway configuration if the same channel width is maintained. This increases the potential for downstream flooding. The staged labyrinth weir is effective at decreasing the detention volume required to pass extreme flood event, but can maintain peak outflows that are approximately equal or less than the capacity of the previous spillway (e.g. ogee crest in this example) for higher-frequency return period storm events.

Staged labyrinth weirs are not useful in every situation, but the design can be beneficial if additional spillway capacity is required for extreme events while meeting discharge requirements for smaller flood events. In some cases downstream flooding may be necessary to safely pass larger flood events without dam failure.

Labyrinth Weir Hydraulics with Angled Approach Flow

This study investigated the potential decrease in efficiency of a labyrinth weir when used with an angled approach flow channel. This configuration is fairly common, as structural requirements may prevent the spillway from being placed in an ideal configuration with perpendicular approach flow. Three different channel angles were tested, including perpendicular to the weir ($\beta = 0°$), at the limit described by Tullis et al. (1995) ($\beta = 15°$), and at an extreme angle ($\beta = 45°$). The results validated the guideline set by Tullis et al. (1995), showing that there was no measureable decrease in efficiency at this approach angle. As β was increased, the discharge coefficient C_d was reduced by as much as 11%. More extreme values in model prototype structures tested reduced C_d even further.

REFERENCES

Amanian, N. (1987). "Performance and design of labyrinth spillway." M.Sc. thesis, Utah State University, Logan, UT.

Anderson, R.M. (2011). "Piano key weir head discharge relationships." M.Sc. thesis, Utah State University, Logan, UT.

Anderson, R.M., and Tullis, B.P. (2012). "Comparison of piano key and rectangular labyrinth weir hydraulics." *J. Hydraul. Eng.*, ASCE, 138(4), 358–361.

Bazin, H. (1894). "Experiences nouvelles sur l'ecoulement en deversoir." *Ann. Ponts Chaussees*, 7(7), 249–357.

Belaabed, F., and Ouamane, A. (2011). "Contribution to the study of the piano key weirs submerged by the downstream level." *Proc., Int. Conf. Labyrinth and Piano Key Weirs–PKW 2011*, Taylor & Francis, London, 89–95.

Campbell and Binder. (1991). "Potential changes in dam owner liability must be considered before modifications are made." Technical review, ASDSO newsletter, 7(1) 7-8.

Cox, G.N. (1928). "The submerged weir as a measuring device." *Bulletin engineering experiment station series No. 67*, Univ. of Wisconsin, Madison, WI.

Crookston, B.M. (2010). "Labyrinth weirs." Ph.D. dissertation, Utah State University, Logan, UT.

Crookston, B.M., and Tullis, B.P. (2012a). "Arced labyrinth weirs." *J. Hydraul. Eng.*, ASCE, 138(6) 555-562.

Crookston, B.M., and Tullis, B.P. (2012b). "Discharge efficiency of reservoir-application- specific labyrinth weirs." *J. Irrig. Drain. Eng.*, ASCE, 138(6) 564-568.

Crookston, B.M., and Tullis, B.P. (2013a). "Hydraulic design and analysis of labyrinth weirs. I: Discharge relationships." *J. Irrig. Drain. Eng.*, ASCE, 139(5), 363-370.

Crookston, B.M., and Tullis, B.P. (2013b). "Hydraulic design and analysis of labyrinth weirs. II: Nappe aeration, instability, and vibration." *J. Irrig. Drain. Eng.*, ASCE, 139(5), 371-377.

Darvas, L. (1971). "Discussion of performance and design of labyrinth weirs," *J. Hydraul. Eng.*, ASCE, 97(80): 1246-1251.

Falvey, H. (2003). *Hydraulic design of labyrinth weirs*. ASCE, Reston, VA.

Francis, J.B. (1884). “Experiments on the flow of water over submerged weirs.” *J. Trans. Eng.*, ASCE, 13(1), 303–312.

Fteley, A., and Stearns, F.P. (1883). “Description of some experiments on flow of water made during the construction of works for conveying water of Sudbury River to Boston.” *J. Trans. Eng.*, ASCE, 12(1), 101–108.

Haestad Methods Engineering Staff. (2002). “Computer applications in hydraulic engineering.” *Detention pond design*, Bentley Institute Press, Exton, PA, 171-174.

Hay, N., and Taylor, G. (1970). “Performance and design of labyrinth weirs.” *J. Hydraul. Eng.*, ASCE, 96(11), 2337-2357.

Henderson, F.M. (1966). “Open channel flow.” *Channel controls*, MacMillan, New York, 174–176.

Hinchliff, D., and Houston, K. (1984). “Hydraulic design and application of labyrinth spillways.” *Proc., 4th Annual USCOLD Lecture*. Dam safety and Rehabilitation, Bureau of Reclamation, U.S. Dept. of the Interior, Washington, DC.

Ho Ta Khanh, M., Sy Quat, D., and Xuan Thuy, D. (2011). “P.K. weirs under design and construction in Vietnam (2010).” *Proc., Int. Conf. Labyrinth and Piano Key Weirs–PKW 2011*, Taylor & Francis, London, 225–232.

Johnson, M.C. (2000). “Discharge coefficient analysis for flat-topped and sharp-crested weirs.” *Irrig. Sci.* 19(3), 133-137.

Laugier, F. (2007). “Design and construction of the first piano key weir spillway at Goulours Dam.” *Int. J. of Hydropower Dams*, 14(5), 94–100.

Lempérière, F. (2009). “New labyrinth weirs triple the spillways discharge.” <http://www.hydrocoop.org> (Aug. 29, 2011).

Lux III, F. and Hinchliff, D. (1985). “Design and construction of labyrinth spillways.” *Proc., 15th Congress ICOLD, Vol. IV*, Q59-R15, Paris, France, 249-274.

Magalhães, A., and Lorena, M. (1989). “Hydraulic design of labyrinth weirs.” *Report No. 736*, National Laboratory of Civil Engineering, Lisbon, Portugal.

Melo, J., Ramos, C., and Magalhães, A. (2002). “Descarregadores com soleira em labirinto de um ciclo em canais convergentes. Determinação da capacidad de vazão.” *Proc. 6° Congresso da Água*, (CD-ROM), Porto, Portugal. (in Portuguese).

Paxson, G.S., and Binder (2009). "The balancing act: considering flooding impacts in design of spillway capacity upgrades." *Annual Conf. Proc.*, ASDSO, Hollywood, FL, 142-149.

Paxson, G.S., Campbell, D., and Monroe, J. (2011). "Evolving design approaches and considerations for labyrinth spillways." *Proc., 31st Annual USSD Conf.* (CD-ROM), San Diego, CA, USA.

Pralong, J., et al. (2011). "A naming convention for the piano key weirs geometrical parameters." *Proc., Int. Conf. Labyrinth and Piano Key Weirs–PKW 2011*, Taylor & Francis, London, 271–278.

Tullis, B.P., Young, J., and Chandler, M. (2007). "Head-discharge relationships for submerged labyrinth weirs." *J. Hydraul. Eng.*, ASCE, 133(3), 248-254.

Tullis, P., Amanian, N., and Waldron, D. (1995). "Design of labyrinth weir spillways." *J. Hydraul. Eng.*, ASCE, 121(3), 247-255.

United States Bureau of Reclamation (USBR). (1987). *Design of Small Dams*. Department of the Interior, Washington, DC, 368.

Villemonte, J. R. (1947). "Submerged weir discharge studies." *Eng. News-Record*, 139(26), 54–57.

Willmore, C. M. (2004). "Hydraulic characteristics of labyrinth weirs." M.Sc. report, Utah State University, Logan, UT.

APPENDICES

Appendix A – Submerged Piano Key Weir Data

Table A1. PKst – $H_t/P = 0.2$

W 36.92 (in) P 7.75 (in) L 186.83 (in)

Run (#)	Q (cfs)	h (ft)	U.S.Vel. (ft/s)	H_t (ft)	H^* (ft)	H_t/P	h_d (ft)	D.S.Vel. (ft/s)	H_d (ft)	H_d/H_t	H^*/H_t	H_d/H^*
1	2	3	4	5	6	7	8	9	10	11	12	13
1	1.871	0.128	0.572	0.133	0.133	0.206	0.132	0.781	0.142		1.000	1.067
2	1.871	0.127	0.572	0.133	0.132	0.206	0.019	0.915	0.032	0.239	0.996	0.240
3	1.871	0.129	0.572	0.133	0.134	0.206	0.039	0.888	0.052	0.388	1.007	0.385
4	1.871	0.132	0.570	0.133	0.137	0.206	0.060	0.862	0.071	0.537	1.030	0.521
5	1.867	0.137	0.566	0.133	0.142	0.206	0.079	0.837	0.090	0.675	1.071	0.630
6	1.871	0.146	0.563	0.133	0.151	0.206	0.099	0.816	0.110	0.825	1.134	0.727
7	1.867	0.158	0.555	0.133	0.163	0.206	0.118	0.794	0.128	0.964	1.224	0.788
8	1.867	0.171	0.548	0.133	0.176	0.206	0.138	0.774	0.147	1.107	1.324	0.836
9	1.871	0.201	0.535	0.133	0.205	0.206	0.175	0.741	0.183	1.380	1.545	0.893
10	1.867	0.232	0.520	0.133	0.236	0.206	0.211	0.708	0.219	1.645	1.776	0.926
11	1.867	0.279	0.500	0.133	0.283	0.206	0.264	0.667	0.271	2.037	2.131	0.956
12	1.863	0.327	0.480	0.133	0.331	0.206	0.314	0.631	0.320	2.412	2.490	0.969
13	1.863	0.375	0.462	0.133	0.378	0.206	0.363	0.600	0.369	2.776	2.846	0.976
14	1.859	0.434	0.441	0.133	0.437	0.206	0.425	0.564	0.430	3.234	3.287	0.984
15	1.855	0.503	0.419	0.133	0.506	0.206	0.496	0.528	0.501	3.768	3.805	0.990
16	1.863	0.374	0.463	0.133	0.377	0.206	0.364	0.600	0.369	2.780	2.838	0.979
17	1.867	0.201	0.534	0.133	0.205	0.206	0.175	0.739	0.184	1.383	1.545	0.895
18	1.871	0.137	0.567	0.133	0.142	0.206	0.079	0.839	0.090	0.675	1.067	0.633

Table A2. PKst – $H_t/P = 0.4$

W 36.92 (in) P 7.75 (in) L 186.83 (in)

Run (#)	Q (cfs)	h (ft)	U.S.Vel. (ft/s)	H_t (ft)	H^* (ft)	H_t/P	h_d (ft)	D.S.Vel. (ft/s)	H_d (ft)	H_d/H_t	H^*/H_t	H_d/H^*
1	2	3	4	5	6	7	8	9	10	11	12	13
1	3.678	0.242	1.016	0.258	0.258	0.399	--	--	--	--	--	--
2	3.678	0.238	1.019	0.258	0.254	0.399	0.047	1.726	0.093	0.361	0.987	0.366
3	3.680	0.239	1.018	0.258	0.255	0.399	0.069	1.674	0.112	0.436	0.991	0.440
4	3.678	0.242	1.016	0.258	0.258	0.399	0.093	1.618	0.133	0.518	1.000	0.518
5	3.676	0.247	1.011	0.258	0.263	0.399	0.114	1.573	0.152	0.590	1.019	0.579
6	3.678	0.263	0.997	0.258	0.279	0.399	0.157	1.489	0.191	0.742	1.081	0.686
7	3.678	0.285	0.980	0.258	0.300	0.399	0.199	1.414	0.230	0.894	1.162	0.769
8	3.672	0.309	0.959	0.258	0.323	0.399	0.240	1.348	0.268	1.040	1.253	0.829
9	3.672	0.337	0.938	0.258	0.350	0.399	0.279	1.290	0.305	1.184	1.359	0.871
10	3.670	0.366	0.917	0.258	0.379	0.399	0.316	1.240	0.340	1.318	1.469	0.897
11	3.668	0.411	0.886	0.258	0.423	0.399	0.371	1.173	0.392	1.521	1.641	0.927
12	3.662	0.518	0.819	0.258	0.529	0.399	0.492	1.046	0.509	1.975	2.051	0.963
13	3.659	0.579	0.785	0.258	0.588	0.399	0.557	0.989	0.572	2.219	2.282	0.972
14	3.666	0.637	0.758	0.258	0.646	0.399	0.619	0.942	0.633	2.456	2.505	0.980
15	3.661	0.692	0.731	0.258	0.700	0.399	0.676	0.900	0.688	2.670	2.716	0.983
16	3.661	0.576	0.787	0.258	0.586	0.399	0.556	0.990	0.571	2.215	2.273	0.975
17	3.676	0.365	0.919	0.258	0.378	0.399	0.316	1.242	0.340	1.318	1.468	0.898
18	3.664	0.263	0.994	0.258	0.279	0.399	0.158	1.482	0.192	0.744	1.081	0.689

Table A3. PKst – $H_t/P = 0.6$

W 36.92 (in) P 7.75 (in) L 186.83 (in)

Run (#)	Q (cfs)	h (ft)	U.S.Vel. (ft/s)	H_t (ft)	H^* (ft)	H_t/P	h_d (ft)	D.S.Vel. (ft/s)	H_d (ft)	H_d/H_t	H^*/H_t	H_d/H^*
1	2	3	4	5	6	7	8	9	10	11	12	13
1	5.530	0.358	1.389	0.388	0.388	0.601	-0.525	20.949	6.289	--	1.000	16.198
2	5.538	0.358	1.392	0.388	0.388	0.601	-0.040	2.972	0.097	0.250	0.999	0.250
3	5.543	0.358	1.393	0.388	0.388	0.601	-0.018	2.868	0.110	0.283	1.000	0.283
4	5.534	0.358	1.391	0.388	0.388	0.601	0.004	2.769	0.123	0.316	1.000	0.316
5	5.534	0.357	1.392	0.388	0.387	0.601	0.029	2.666	0.139	0.358	0.998	0.359
6	5.530	0.360	1.388	0.388	0.390	0.601	0.054	2.567	0.157	0.403	1.004	0.402
7	5.534	0.360	1.389	0.388	0.390	0.601	0.078	2.486	0.174	0.447	1.004	0.446
8	5.538	0.366	1.384	0.388	0.396	0.601	0.124	2.339	0.209	0.538	1.019	0.528
9	5.538	0.370	1.379	0.388	0.399	0.601	0.170	2.207	0.245	0.632	1.029	0.615
10	5.538	0.379	1.370	0.388	0.408	0.601	0.214	2.094	0.282	0.726	1.051	0.691
11	5.538	0.402	1.346	0.388	0.430	0.601	0.277	1.951	0.336	0.865	1.107	0.781
12	5.530	0.438	1.309	0.388	0.464	0.601	0.338	1.827	0.390	1.004	1.196	0.839
13	5.525	0.479	1.270	0.388	0.504	0.601	0.396	1.724	0.442	1.138	1.298	0.877
14	5.525	0.521	1.233	0.388	0.545	0.601	0.452	1.635	0.494	1.272	1.403	0.906
15	5.517	0.567	1.194	0.388	0.589	0.601	0.510	1.552	0.547	1.409	1.517	0.929
16	5.512	0.610	1.160	0.388	0.631	0.601	0.564	1.481	0.598	1.540	1.624	0.948
17	5.504	0.672	1.113	0.388	0.691	0.601	0.632	1.400	0.662	1.706	1.780	0.958
18	5.495	0.731	1.072	0.388	0.749	0.601	0.698	1.329	0.726	1.869	1.928	0.969
19	5.504	0.670	1.115	0.388	0.689	0.601	0.632	1.400	0.662	1.706	1.775	0.961
20	5.521	0.523	1.230	0.388	0.547	0.601	0.456	1.628	0.497	1.281	1.408	0.910
21	5.538	0.377	1.372	0.388	0.406	0.601	0.210	2.103	0.279	0.718	1.046	0.687

Table A4. PKmod – $H_t/P = 0.2$

W 36.92 (in) P 8.75 (in) L 186.89 (in)

Run (#)	Q (cfs)	h (ft)	U.S.Vel. (ft/s)	H_t (ft)	H^* (ft)	H_t/P	h_d (ft)	D.S.Vel. (ft/s)	H_d (ft)	H_d/H_t	H^*/H_t	H_d/H^*
1	2	3	4	5	6	7	8	9	10	11	12	13
1	2.380	0.143	0.666	0.150	0.150	0.206	--	--	--	--	--	--
2	2.380	0.143	0.666	0.150	0.150	0.206	0.018	1.035	0.035	0.233	0.997	0.233
3	2.377	0.149	0.661	0.150	0.156	0.206	0.057	0.982	0.072	0.481	1.039	0.463
4	2.374	0.155	0.657	0.150	0.162	0.206	0.079	0.954	0.093	0.622	1.079	0.577
5	2.377	0.156	0.658	0.150	0.163	0.206	0.079	0.956	0.093	0.622	1.082	0.575
6	2.374	0.174	0.647	0.150	0.181	0.206	0.118	0.910	0.131	0.873	1.204	0.726
7	2.374	0.201	0.632	0.150	0.208	0.206	0.155	0.872	0.167	1.113	1.382	0.805
8	2.371	0.229	0.617	0.150	0.235	0.206	0.192	0.836	0.203	1.353	1.566	0.864
9	2.368	0.258	0.603	0.150	0.264	0.206	0.224	0.807	0.234	1.561	1.758	0.888
10	2.371	0.259	0.603	0.150	0.265	0.206	0.227	0.806	0.237	1.581	1.764	0.896
11	2.365	0.304	0.581	0.150	0.310	0.206	0.278	0.763	0.287	1.913	2.061	0.928
12	2.362	0.349	0.561	0.150	0.354	0.206	0.328	0.726	0.336	2.241	2.355	0.951
13	2.362	0.393	0.544	0.150	0.398	0.206	0.376	0.694	0.384	2.556	2.649	0.965
14	2.359	0.452	0.521	0.150	0.457	0.206	0.438	0.657	0.445	2.963	3.040	0.975
15	2.356	0.499	0.504	0.150	0.503	0.206	0.487	0.629	0.493	3.286	3.351	0.981
16	2.356	0.503	0.503	0.150	0.507	0.206	0.491	0.627	0.497	3.312	3.378	0.981
17	2.356	0.556	0.486	0.150	0.560	0.206	0.545	0.601	0.551	3.668	3.729	0.984
18	2.352	0.603	0.472	0.150	0.606	0.206	0.594	0.578	0.599	3.992	4.037	0.989

Table A5. PKmod – $H_t/P = 0.4$

W 36.92 (in) P 8.75 (in) L 186.89 (in)

Run (#)	Q (cfs)	h (ft)	U.S.Vel. (ft/s)	H_t (ft)	H^* (ft)	H_t/P	h_d (ft)	D.S.Vel. (ft/s)	H_d (ft)	H_d/H_t	H^*/H_t	H_d/H^*
1	2	3	4	5	6	7	8	9	10	11	12	13
31	4.688	0.268	1.184	0.290	0.290	0.397	--	--	--	--	--	--
32	4.684	0.267	1.184	0.290	0.289	0.397	--	--	--	--	--	--
1	4.680	0.264	1.185	0.290	0.286	0.397	-0.029	2.173	0.044	0.152	0.988	0.154
2	4.678	0.264	1.185	0.290	0.286	0.397	-0.004	2.096	0.064	0.223	0.988	0.225
3	4.684	0.266	1.185	0.290	0.288	0.397	0.026	2.015	0.089	0.309	0.995	0.310
4	4.678	0.266	1.184	0.290	0.288	0.397	0.033	1.994	0.095	0.328	0.993	0.330
5	4.684	0.268	1.183	0.290	0.290	0.397	0.054	1.943	0.113	0.390	1.002	0.389
6	4.674	0.269	1.179	0.290	0.291	0.397	0.069	1.902	0.125	0.433	1.005	0.431
7	4.722	0.275	1.186	0.290	0.297	0.397	0.089	1.875	0.144	0.497	1.026	0.484
8	4.686	0.275	1.177	0.290	0.297	0.397	0.104	1.828	0.156	0.538	1.025	0.525
9	4.686	0.292	1.162	0.290	0.313	0.397	0.140	1.752	0.188	0.649	1.082	0.600
10	4.690	0.307	1.150	0.290	0.328	0.397	0.174	1.687	0.218	0.755	1.132	0.667
11	4.692	0.334	1.127	0.290	0.354	0.397	0.224	1.599	0.264	0.912	1.223	0.746
12	4.714	0.363	1.109	0.290	0.382	0.397	0.267	1.538	0.304	1.050	1.320	0.795
13	4.688	0.364	1.102	0.290	0.383	0.397	0.270	1.524	0.306	1.058	1.323	0.800
14	4.688	0.365	1.101	0.290	0.384	0.397	0.272	1.522	0.308	1.063	1.326	0.801
15	4.686	0.398	1.075	0.290	0.416	0.397	0.318	1.454	0.351	1.213	1.436	0.845
16	4.684	0.426	1.053	0.290	0.444	0.397	0.355	1.404	0.386	1.333	1.532	0.870
17	4.680	0.454	1.033	0.290	0.471	0.397	0.392	1.356	0.421	1.453	1.626	0.894
18	4.678	0.483	1.012	0.290	0.499	0.397	0.428	1.313	0.455	1.572	1.724	0.912
19	4.674	0.511	0.993	0.290	0.527	0.397	0.461	1.276	0.487	1.680	1.819	0.924
20	4.669	0.539	0.974	0.290	0.554	0.397	0.495	1.239	0.519	1.793	1.913	0.937
21	4.680	0.570	0.957	0.290	0.584	0.397	0.528	1.210	0.551	1.903	2.017	0.943
22	4.678	0.597	0.941	0.290	0.611	0.397	0.560	1.179	0.582	2.009	2.110	0.952
23	4.680	0.618	0.929	0.290	0.632	0.397	0.583	1.159	0.604	2.086	2.181	0.956
24	4.694	0.626	0.927	0.290	0.640	0.397	0.591	1.155	0.612	2.114	2.209	0.957
25	4.688	0.626	0.926	0.290	0.640	0.397	0.593	1.152	0.614	2.120	2.209	0.960
26	4.684	0.659	0.907	0.290	0.672	0.397	0.626	1.123	0.646	2.230	2.319	0.962
27	4.678	0.710	0.880	0.290	0.722	0.397	0.683	1.077	0.701	2.420	2.493	0.971
28	4.674	0.758	0.855	0.290	0.770	0.397	0.734	1.038	0.751	2.594	2.658	0.976
29	4.684	0.807	0.834	0.290	0.818	0.397	0.786	1.004	0.802	2.769	2.825	0.980
30	4.684	0.828	0.824	0.290	0.838	0.397	0.808	0.990	0.824	2.844	2.895	0.982

Table A6. PKmod – $H_t/P = 0.6$

W 36.92 (in) P 8.75 (in) L 186.89 (in)

Run (#)	Q (cfs)	h (ft)	U.S.Vel. (ft/s)	H_t (ft)	H^* (ft)	H_t/P	h_d (ft)	D.S.Vel. (ft/s)	H_d (ft)	H_d/H_t	H^*/H_t	H_d/H^*
1	2	3	4	5	6	7	8	9	10	11	12	13
1	6.881	0.395	1.582	0.434	0.434	0.595	--	--	--	--	--	--
2	6.881	0.402	1.574	0.434	0.441	0.595	0.114	2.652	0.223	0.515	1.015	0.507
3	6.867	0.408	1.564	0.434	0.446	0.595	0.159	2.512	0.257	0.593	1.028	0.577
4	6.881	0.423	1.551	0.434	0.461	0.595	0.223	2.348	0.309	0.712	1.061	0.671
5	6.878	0.450	1.522	0.434	0.486	0.595	0.286	2.201	0.362	0.833	1.120	0.744
6	6.863	0.434	1.535	0.434	0.471	0.595	0.256	2.263	0.336	0.774	1.085	0.713
7	6.859	0.479	1.489	0.434	0.513	0.595	0.333	2.098	0.402	0.925	1.182	0.783
8	6.866	0.518	1.452	0.434	0.551	0.595	0.388	1.997	0.450	1.037	1.269	0.817
9	6.859	0.568	1.405	0.434	0.599	0.595	0.463	1.870	0.518	1.192	1.380	0.864
10	6.852	0.624	1.356	0.434	0.653	0.595	0.535	1.761	0.583	1.344	1.504	0.894
11	6.856	0.680	1.312	0.434	0.707	0.595	0.605	1.670	0.649	1.494	1.629	0.917
12	6.863	0.738	1.270	0.434	0.763	0.595	0.675	1.588	0.714	1.646	1.758	0.936
13	6.845	0.845	1.194	0.434	0.867	0.595	0.800	1.455	0.833	1.919	1.998	0.960
14	6.863	0.735	1.272	0.434	0.760	0.595	0.676	1.587	0.715	1.648	1.752	0.941
15	6.845	0.510	1.455	0.434	0.543	0.595	0.378	2.009	0.441	1.016	1.251	0.812
16	6.856	0.422	1.546	0.434	0.459	0.595	0.226	2.332	0.311	0.716	1.058	0.676

Appendix B – Staged Labyrinth Weir Data

Table B1. Data for Model 1a

P	0.50	(ft)
P'	0.40	(ft)
N	4	

L	156.80	(in)
l_{stage}	2.90	(in)

t	0.75	(in)
W	48.41	(in)

Run (#)	Q (cfs)	H (ft)	H' (ft)	U.S. Vel. (ft/s)	H_t (ft)	H_t' (ft)	H_t/P	H_t'/P'	C_d	Stage
1	2	3	4	5	6	7	8	9	10	13
1	0.011	--	0.069	0.004	--	0.069	--	0.174	--	Low
2	0.019	--	0.092	0.006	--	0.092	--	0.231	--	Low
3	0.461	0.050	0.150	0.132	0.050	0.150	0.100	0.376	0.586	Both
4	0.607	0.060	0.160	0.172	0.060	0.160	0.121	0.401	0.585	Both
5	0.881	0.076	0.176	0.246	0.077	0.177	0.155	0.443	0.586	Both
6	0.886	0.077	0.175	0.247	0.078	0.176	0.156	0.440	0.583	Both
7	1.213	0.095	0.195	0.331	0.097	0.197	0.193	0.492	0.578	Both
8	1.271	0.098	0.196	0.346	0.100	0.198	0.200	0.494	0.577	Both
9	1.585	0.114	0.214	0.424	0.117	0.217	0.233	0.542	0.569	Both
10	1.983	0.133	0.233	0.520	0.138	0.238	0.275	0.594	0.556	Both
11	2.311	0.149	0.247	0.595	0.155	0.253	0.310	0.632	0.542	Both
12	2.405	0.153	0.251	0.617	0.159	0.257	0.319	0.643	0.541	Both
13	2.545	0.159	0.259	0.649	0.166	0.266	0.332	0.665	0.539	Both
14	3.745	0.215	0.315	0.903	0.228	0.328	0.455	0.819	0.493	Both
15	3.794	0.222	0.320	0.909	0.235	0.333	0.469	0.832	0.477	Both
16	3.988	0.233	0.331	0.945	0.247	0.345	0.495	0.863	0.464	Both
17	4.769	0.272	0.372	1.090	0.290	0.390	0.581	0.976	0.436	Both
18	6.019	0.347	0.445	1.287	0.373	0.471	0.745	1.177	0.379	Both
19	8.142	0.462	0.560	1.583	0.501	0.599	1.003	1.498	0.328	Both
20	9.973	0.560	0.658	1.801	0.610	0.708	1.221	1.771	0.299	Both
21	10.637	0.594	0.692	1.875	0.649	0.746	1.297	1.866	0.291	Both
22	11.003	0.611	0.711	1.916	0.668	0.768	1.336	1.920	0.288	Both
23	17.035	0.884	0.984	2.489	0.980	1.080	1.960	2.701	0.251	Both
24	17.360	0.898	0.996	2.515	0.997	1.095	1.993	2.737	0.250	Both

Table B2. Data for Model 1b

P	0.50	(ft)
P'	0.45	(ft)
N	4	

L	156.80	(in)
l_{stage}	2.90	(in)

t	0.75	(in)
W	48.41	(in)

Run (#)	Q (cfs)	H (ft)	H' (ft)	U.S. Vel. (ft/s)	H_t (ft)	H_t' (ft)	H_t/P	H_t'/P'	C_d	Stage
1	2	3	4	5	6	7	8	9	10	13
1	0.003	--	0.026	0.001	--	0.026	--	0.058	--	Low
2	0.007	--	0.048	0.002	--	0.048	--	0.107	--	Low
3	0.009	--	0.054	0.003	--	0.054	--	0.120	--	Low
4	0.436	0.050	0.100	0.125	0.051	0.051	0.101	0.113	0.547	Both
5	0.435	0.051	0.101	0.125	0.051	0.051	0.102	0.114	0.537	Both
6	0.487	0.054	0.104	0.139	0.055	0.055	0.109	0.122	0.544	Both
7	0.565	0.059	0.109	0.161	0.060	0.060	0.120	0.133	0.552	Both
8	0.705	0.068	0.118	0.199	0.069	0.069	0.138	0.153	0.556	Both
9	0.819	0.075	0.125	0.229	0.076	0.076	0.153	0.169	0.556	Both
10	1.139	0.093	0.143	0.312	0.095	0.095	0.190	0.211	0.557	Both
11	1.237	0.099	0.149	0.336	0.101	0.101	0.201	0.224	0.554	Both
12	1.566	0.115	0.165	0.418	0.118	0.118	0.236	0.263	0.552	Both
13	1.923	0.133	0.183	0.504	0.137	0.137	0.274	0.304	0.543	Both
14	2.575	0.162	0.212	0.655	0.169	0.169	0.338	0.376	0.530	Both
15	2.598	0.164	0.214	0.659	0.171	0.171	0.341	0.379	0.527	Both
16	3.181	0.190	0.240	0.787	0.200	0.200	0.399	0.443	0.511	Both
17	3.665	0.214	0.264	0.885	0.226	0.226	0.452	0.502	0.488	Both
18	3.996	0.230	0.280	0.950	0.244	0.244	0.488	0.542	0.475	Both
19	4.142	0.236	0.286	0.979	0.251	0.251	0.502	0.557	0.472	Both
20	4.797	0.274	0.324	1.094	0.293	0.293	0.586	0.651	0.433	Both
21	5.535	0.314	0.364	1.218	0.337	0.337	0.675	0.750	0.404	Both
22	8.606	0.477	0.527	1.654	0.519	0.519	1.039	1.154	0.329	Both
23	9.176	0.509	0.559	1.721	0.555	0.555	1.110	1.233	0.318	Both
24	20.361	1.002	1.052	2.782	1.122	1.122	2.244	2.494	0.245	Both

P	0.50	(ft)	L	156.80	(in)	t	0.75	(in)
P'	0.40	(ft)	l_{stage}	9.16	(in)	W	48.41	(in)
N	4							

Run (#)	Q (cfs)	H (ft)	H' (ft)	U.S. Vel. (ft/s)	H_t (ft)	H_t' (ft)	H_t/P	H_t'/P'	C_d	Stage
1	2	3	4	5	6	7	8	9	10	13
1	0.014	--	0.034	0.005	--	0.034	--	0.086	--	low
3	0.044	--	0.074	0.014	--	0.074	--	0.184	--	low
2	0.067	--	0.104	0.020	--	0.104	--	0.261	--	low
6	0.572	0.052	0.156	0.164	0.053	0.156	0.106	0.390	0.674	both
7	0.615	0.055	0.159	0.176	0.056	0.159	0.112	0.398	0.666	both
8	0.793	0.066	0.170	0.224	0.067	0.171	0.134	0.426	0.651	both
9	0.942	0.075	0.179	0.263	0.077	0.180	0.153	0.450	0.637	both
10	1.258	0.093	0.197	0.344	0.095	0.199	0.191	0.496	0.612	both
11	1.779	0.118	0.222	0.474	0.122	0.225	0.244	0.563	0.598	both
12	2.305	0.144	0.248	0.597	0.150	0.253	0.300	0.633	0.568	both
13	2.757	0.165	0.269	0.699	0.173	0.276	0.346	0.691	0.548	both
14	3.543	0.201	0.304	0.867	0.213	0.316	0.425	0.790	0.517	both
15	4.157	0.232	0.336	0.986	0.248	0.351	0.495	0.877	0.483	both
16	4.205	0.237	0.340	0.993	0.252	0.356	0.505	0.889	0.475	both
17	4.244	0.238	0.342	1.001	0.254	0.357	0.508	0.893	0.474	both
18	5.160	0.289	0.393	1.161	0.310	0.414	0.621	1.034	0.427	both
19	6.881	0.383	0.486	1.427	0.415	0.518	0.829	1.295	0.369	both
20	8.326	0.461	0.564	1.621	0.502	0.605	1.003	1.513	0.335	both
21	9.641	0.526	0.630	1.785	0.576	0.679	1.152	1.698	0.316	both
22	17.246	0.884	0.988	2.519	0.983	1.086	1.966	2.716	0.253	both

Table B3. Data for Model 2

Table B4. Data for Model 3

P	0.50	(ft)
P'	0.40	(ft)
N	4	

L	156.80	(in)
l_{stage}	9.16	(in)

t	0.75	(in)
W	48.41	(in)

Run (#)	Q (cfs)	H (ft)	H' (ft)	U.S. Vel. (ft/s)	H_t (ft)	H_t' (ft)	H_t/P	H_t'/P'	C_d	Stage
1	2	3	4	5	6	7	8	9	10	13
1	0.015	--	0.037	0.005	--	0.037	--	0.091	--	low
2	0.039	--	0.062	0.012	--	0.062	--	0.154	--	low
3	0.088	--	0.103	0.027	--	0.103	--	0.258	--	low
5	0.611	0.051	0.155	0.175	0.051	0.155	0.103	0.387	0.753	both
6	0.865	0.066	0.170	0.244	0.067	0.171	0.134	0.427	0.711	both
7	1.109	0.080	0.184	0.308	0.082	0.185	0.164	0.464	0.679	both
8	1.359	0.093	0.197	0.372	0.095	0.199	0.191	0.498	0.660	both
9	1.776	0.115	0.219	0.475	0.118	0.222	0.237	0.555	0.625	both
10	2.345	0.142	0.246	0.609	0.148	0.251	0.295	0.628	0.592	both
11	2.911	0.168	0.272	0.736	0.177	0.280	0.353	0.701	0.561	both
12	3.900	0.218	0.322	0.938	0.231	0.335	0.463	0.838	0.501	both
13	4.013	0.224	0.328	0.959	0.239	0.342	0.477	0.856	0.493	both
14	4.290	0.238	0.342	1.012	0.254	0.357	0.507	0.894	0.480	both
15	4.499	0.249	0.353	1.050	0.266	0.370	0.533	0.925	0.468	both
16	5.372	0.299	0.403	1.198	0.321	0.425	0.642	1.062	0.423	both
17	6.518	0.362	0.466	1.376	0.391	0.495	0.782	1.237	0.381	both
18	7.481	0.415	0.519	1.511	0.450	0.554	0.901	1.385	0.354	both
19	8.267	0.456	0.560	1.616	0.496	0.600	0.993	1.500	0.338	both
20	10.032	0.545	0.649	1.832	0.597	0.701	1.194	1.752	0.311	both
21	17.586	0.895	0.999	2.552	0.997	1.100	1.993	2.751	0.253	both

Table B5. Data for Model 4

P	0.50	(ft)
P'	0.40	(ft)
N	4	

L	156.80	(in)
l_{stage}	9.16	(in)

t	0.75	(in)
W	48.41	(in)

Run (#)	Q (cfs)	H (ft)	H' (ft)	U.S. Vel. (ft/s)	H_t (ft)	H_t' (ft)	H_t/P	H_t'/P'	C_d	Stage
1	2	3	4	5	6	7	8	9	10	13
1	0.013	--	0.031	0.004	--	0.031	--	0.077	--	low
2	0.028	--	0.055	0.009	--	0.055	--	0.137	--	low
3	0.046	--	0.078	0.014	--	0.078	--	0.196	--	low
4	0.578	0.051	0.153	0.166	0.051	0.153	0.103	0.383	0.710	both
5	0.584	0.052	0.154	0.167	0.053	0.155	0.106	0.387	0.687	both
6	0.796	0.065	0.167	0.225	0.066	0.168	0.132	0.420	0.668	both
7	0.988	0.077	0.179	0.275	0.078	0.180	0.156	0.450	0.647	both
8	1.195	0.089	0.191	0.329	0.091	0.192	0.181	0.481	0.627	both
9	1.350	0.097	0.199	0.368	0.099	0.201	0.198	0.502	0.620	both
10	1.723	0.116	0.218	0.460	0.119	0.221	0.239	0.553	0.599	both
11	2.193	0.138	0.240	0.572	0.143	0.245	0.286	0.612	0.580	both
12	2.677	0.159	0.261	0.683	0.166	0.268	0.332	0.670	0.565	both
13	3.096	0.178	0.280	0.775	0.187	0.289	0.375	0.723	0.547	both
14	3.661	0.206	0.308	0.891	0.218	0.320	0.437	0.800	0.514	both
15	4.098	0.230	0.332	0.974	0.245	0.347	0.489	0.866	0.484	both
16	4.205	0.234	0.336	0.996	0.249	0.351	0.499	0.878	0.483	both
17	4.586	0.258	0.360	1.062	0.275	0.377	0.551	0.943	0.454	both
18	6.513	0.372	0.474	1.363	0.401	0.503	0.802	1.257	0.367	both
19	8.342	0.460	0.562	1.624	0.501	0.603	1.003	1.508	0.336	both
20	9.322	0.510	0.612	1.747	0.558	0.660	1.116	1.649	0.320	both
21	13.908	0.730	0.832	2.234	0.808	0.910	1.616	2.275	0.274	both

Table B6. Data for Model 5

P	0.50	(ft)
P'	0.40	(ft)
N	4	

L	156.80	(in)
l_{stage}	39.20	(in)

t	0.75	(in)
W	48.41	(in)

Run (#)	Q (cfs)	H (ft)	H' (ft)	U.S. Vel. (ft/s)	H_t (ft)	H_t' (ft)	H_t/P	H_t/P'	C_d	Stage
1	2	3	4	5	6	7	8	9	10	13
1	0.033	--	0.024	0.011	--	0.024	--	0.060	--	Low
2	0.077	--	0.040	0.025	--	0.040	--	0.100	--	Low
3	0.098	--	0.046	0.032	--	0.046	--	0.115	--	Low
4	0.319	--	0.096	0.098	--	0.096	--	0.241	--	Low
5	0.360	--	0.103	0.110	--	0.103	--	0.257	--	Low
6	0.936	0.048	0.152	0.269	0.049	0.153	0.099	0.383	1.219	Both
7	1.237	0.067	0.171	0.349	0.069	0.172	0.137	0.431	0.984	Both
8	1.530	0.084	0.188	0.423	0.087	0.190	0.173	0.476	0.859	Both
9	1.992	0.109	0.213	0.536	0.113	0.217	0.227	0.543	0.748	Both
10	2.498	0.134	0.238	0.654	0.141	0.245	0.282	0.612	0.676	Both
11	3.348	0.174	0.278	0.841	0.185	0.289	0.370	0.721	0.603	Both
12	3.743	0.193	0.297	0.922	0.207	0.310	0.413	0.776	0.571	Both
13	4.134	0.214	0.318	0.998	0.230	0.334	0.460	0.834	0.537	Both
14	4.514	0.235	0.339	1.068	0.253	0.357	0.506	0.892	0.508	Both
15	5.154	0.271	0.375	1.179	0.293	0.397	0.586	0.992	0.465	Both
16	6.052	0.320	0.424	1.324	0.348	0.451	0.695	1.128	0.423	Both
17	7.850	0.416	0.520	1.584	0.455	0.559	0.911	1.398	0.366	Both
18	8.263	0.442	0.546	1.633	0.483	0.587	0.966	1.468	0.352	Both
19	10.052	0.528	0.632	1.858	0.582	0.686	1.164	1.714	0.324	Both
20	13.402	0.700	0.804	2.196	0.775	0.879	1.550	2.198	0.281	Both

Table B7. Data for Model 6

P	0.50	(ft)	t	0.75	(in)
L	156.80	(in)	W	48.41	(in)
N	4				

Run (#)	Q (cfs)	H (ft)	U.S. Vel. (ft/s)	H_t (ft)	H_t/P	C_d
1	2	3	5	6	8	10
1	0.417	0.051	0.120	0.051	0.102	0.516
2	0.420	0.051	0.121	0.052	0.103	0.512
3	0.652	0.067	0.184	0.067	0.135	0.532
4	0.803	0.076	0.224	0.077	0.153	0.541
5	1.054	0.090	0.289	0.091	0.182	0.547
6	1.293	0.103	0.350	0.105	0.210	0.545
7	1.705	0.123	0.452	0.126	0.252	0.545
8	2.364	0.153	0.607	0.159	0.317	0.535
9	2.766	0.172	0.696	0.179	0.359	0.521
10	3.275	0.196	0.805	0.206	0.412	0.501
11	3.670	0.212	0.888	0.224	0.448	0.495
12	3.910	0.225	0.934	0.239	0.478	0.479
13	4.127	0.236	0.975	0.251	0.502	0.469
14	4.892	0.279	1.110	0.299	0.597	0.429
15	6.068	0.344	1.301	0.370	0.740	0.385
16	7.204	0.406	1.465	0.439	0.879	0.354
17	8.506	0.474	1.639	0.516	1.031	0.329
18	8.468	0.474	1.631	0.516	1.032	0.327
19	9.800	0.539	1.797	0.590	1.179	0.310
20	13.180	0.700	2.159	0.773	1.546	0.278
21	15.348	0.795	2.367	0.882	1.764	0.265
22	17.883	0.900	2.588	1.005	2.009	0.254
23	20.232	0.994	2.776	1.114	2.227	0.246

Appendix C – Angled Approach Flow Data

Table C1. Data for approach angle $\beta = 0°$

P	0.985	(ft)	t	0.75	(in)
L	156.8	(in)	W	48.41	(in)
N	4				

Run (#)	Q (cfs)	H (ft)	U.S. Vel. (ft/s)	H_t (ft)	H_t/P	C_d
1	6	8	9	10	13	12
1	2.402	0.153	0.523	0.157	0.160	0.550
2	3.363	0.198	0.704	0.206	0.209	0.515
3	4.904	0.274	0.965	0.289	0.293	0.452
4	6.668	0.363	1.226	0.387	0.392	0.397
5	9.700	0.509	1.609	0.549	0.558	0.341
6	12.188	0.612	1.891	0.668	0.678	0.320
7	15.938	0.757	2.268	0.837	0.850	0.298
8	18.287	0.850	2.470	0.945	0.959	0.285
9	16.709	0.790	2.333	0.875	0.888	0.292
10	13.603	0.666	2.042	0.731	0.742	0.311
11	10.798	0.557	1.735	0.604	0.613	0.329
12	10.126	0.529	1.658	0.572	0.581	0.335
13	8.147	0.439	1.418	0.470	0.478	0.361
14	4.101	0.235	0.833	0.246	0.250	0.481
15	0.783	0.072	0.184	0.073	0.074	0.572
16	1.540	0.111	0.348	0.113	0.115	0.580
17	1.158	0.092	0.266	0.093	0.095	0.581
18	1.845	0.126	0.411	0.129	0.131	0.571
19	2.711	0.167	0.583	0.172	0.175	0.542
20	4.650	0.261	0.925	0.274	0.279	0.463
21	0.416	0.050	0.100	0.050	0.051	0.527
22	0.503	0.056	0.120	0.056	0.057	0.537
23	0.584	0.061	0.138	0.061	0.062	0.548

Table C2. Data for approach angle β = 15°

P	0.985	(ft)	t	0.75	(in)
L	156.8	(in)	W	48.41	(in)
N	4				

Run (#)	Q (cfs)	H (ft)	U.S. Vel. (ft/s)	H_t (ft)	H_t/P	C_d
1	6	8	9	10	13	12
1	3.362	0.199	0.523	0.207	0.210	0.511
2	4.742	0.269	0.704	0.283	0.287	0.451
3	6.515	0.361	0.965	0.384	0.389	0.392
4	8.711	0.472	1.226	0.506	0.514	0.346
5	11.622	0.595	1.609	0.647	0.657	0.320
6	15.305	0.748	1.891	0.823	0.835	0.294
7	18.680	0.892	2.268	0.987	1.002	0.273
8	16.192	0.788	2.470	0.868	0.881	0.287
9	8.029	0.438	2.333	0.469	0.476	0.358
10	3.914	0.228	2.042	0.238	0.242	0.482
11	0.276	0.039	1.735	0.039	0.040	0.508
12	0.448	0.052	1.658	0.052	0.053	0.535
13	0.515	0.056	1.418	0.056	0.057	0.550
14	0.613	0.063	0.833	0.063	0.064	0.555
15	0.770	0.072	0.184	0.073	0.074	0.562
16	1.060	0.087	0.348	0.088	0.089	0.580
17	1.400	0.105	0.266	0.107	0.108	0.574
18	1.907	0.129	0.411	0.132	0.134	0.569
19	2.712	0.167	0.583	0.172	0.175	0.542
20	4.226	0.242	0.925	0.254	0.257	0.474

Table C3. Data for approach angle $\beta = 45°$

P	0.985	(ft)	t	0.75	(in)
L	156.8	(in)	W	48.41	(in)
N	4				

Run (#)	Q (cfs)	H (ft)	U.S. Vel. (ft/s)	H_t (ft)	H_t/P	C_d
1	6	8	9	10	13	12
1	2.782	0.173	0.596	0.178	0.181	0.529
2	3.532	0.213	0.731	0.221	0.225	0.485
3	4.402	0.267	0.871	0.279	0.283	0.428
4	4.841	0.292	0.940	0.305	0.310	0.410
5	5.759	0.344	1.074	0.362	0.368	0.378
6	6.789	0.405	1.210	0.428	0.434	0.347
7	7.972	0.472	1.356	0.501	0.508	0.322
8	9.372	0.545	1.518	0.581	0.590	0.303
9	10.663	0.615	1.652	0.658	0.668	0.286
10	15.295	0.814	2.107	0.883	0.897	0.264
11	13.358	0.735	1.925	0.793	0.805	0.271
12	17.611	0.917	2.295	0.999	1.014	0.252
13	3.804	0.228	0.777	0.238	0.241	0.470
14	7.764	0.461	1.331	0.489	0.496	0.325
15	16.901	0.884	2.242	0.962	0.976	0.256
16	0.389	0.047	0.093	0.047	0.048	0.541
17	0.535	0.057	0.127	0.057	0.058	0.556
18	0.673	0.066	0.159	0.066	0.067	0.567
19	1.124	0.091	0.259	0.092	0.094	0.574
20	1.524	0.111	0.345	0.113	0.115	0.574
21	2.206	0.144	0.484	0.148	0.150	0.555
22	2.576	0.163	0.556	0.167	0.170	0.538

Appendix D – Permissions

Permissions Request

As an ASCE author, you are permitted to reuse you own content for another ASCE or non-ASCE publication.

Please add the full credit line "With permission from ASCE" to your source citation. Please print this page for your records.

Type of use: Dissertation/Thesis

Portion: full article

Format: print and electronic

Use of this content will make up more than 25% of the new work: no

Author of this ASCE work or ASCE will publish the new work: yes

BACK | CLOSE WINDOW

Date: April 7th, 2014

Dear Mitchell Dabling:

I give full permission for you to reuse our co-authored publication "Staged Labyrinth Weir Hydraulics," published November 11th, 2013 in the *ASCE Journal of Irrigation and Drainage Engineering*, in your thesis titled "Nonlinear Weir Hydraulics."

Sincerely,

Brian Crookston, PhD, PE
Project Engineer, Schnabel Engineering